THE UNIVERSITY OF QUEENSLAND

Bachelor of Engineering Thesis

Assessing the Potential for CSP Integration with Australia's Coal-Fired Power Plants

Student Name: Joseph SOMERS

Course Code: MECH4500

Supervisor: Professor H. Gurgenci

Submission date: 27 October 2016

A thesis submitted in partial fulfilment of the requirements of the Bachelor of Engineering degree in Mechanical Engineering

Acknowledgements

I wish to thank my undergraduate thesis supervisor, professor Hal Gurgenci, for his support and guidance throughout the year.

Abstract

As a result of the high emission intensity and limited supply of fossil fuels, there is a need for Australia to change its focus to renewable energy solutions that have both abundant free energy sources and produce significantly less greenhouse gas emissions. An article released by Dalvi through publication 'Nature Climate Change' [2], titled 'Thermal Technologies as a Bridge from Fossil Fuels to Renewables', details the potential of integrating solar thermal systems to existing Rankine-cycle power plants with minimal modifications to the existing infrastructure. This thesis report assesses the potential of integrating CSP technology with Australia's coal fired power plants. An analysis is performed on the most appropriate solar to coal integration points, the most useful solar collector type for this application, and the resulting PPA price of solar energy produced from an integrated system. It was determined that electricity produced by solar integration is currently more expensive than electricity produced by coal alone, however, it is far more competitive than stand-alone CSP plants. Furthermore, solar-coal integration was found to significantly reduce the CO_2 emissions of a coal-fired power plant.

Table of Contents

List of Figures

List of Tables

Nomenclature

ARENA	Australian Renewable Energy Agency
BOM	Bureau of Meteorology
BREE	Bureau of Resources and Energy Economics
CO_2	Carbon Dioxide
CSP	Concentrating Solar Power
CST	Concentrating Solar Thermal
DNI	Direct Normal Irradiance
HP	High Pressure
HTF	Heat Transfer Fluid
kWh	Kilo-Watt Hours
IRR	Internal Rate of Return
NGER	National Greenhouse and Energy Reporting
NREL	Nation Renewable Energy Laboratory
MNGSEC	Martin Next Generation Solar Energy Centre
PDC	Parabolic Dish Collector
PPA	Power Purchase Agreement
PTC	Parabolic Trough Collector
SAM	System Advisory Model
SM	Solar Multiple
UV	Ultraviolet

1. Introduction

1.1 Thesis Overview

Fossil fuels such as crude oil, natural gas, and coal currently supply Australia with 86% of our electrical needs [1]. While these fuel sources are comparatively cheap, they are also limited and are being depleted as a result of our society's reliance on power-driven technology. Furthermore, the use of fossil fuels has brought about serious environmental damage, including but not limited to; deforestation, pollution, and the ongoing rise in global atmospheric temperatures. As such, there is a need for Australia to change its focus to renewable energy solutions that have both abundant free energy sources and produce significantly less greenhouse gas emissions when compared to fossil fuels. An article released by Dalvi through publication 'Nature Climate Change' [2], titled 'Thermal Technologies as a Bridge from Fossil Fuels to Renewables', details the potential of integrating solar thermal systems to existing Rankine-cycle power plants with minimal modifications to the existing infrastructure. This thesis report will assess the potential of integrating CSP technology with Australia's coal fired power plants. The economic and environmental effects of integrating CSP will also be determined.

Large-scale Concentrating Solar Thermal (CST) systems would be required to add significant energy production to current coal fired plants in Australia. One such system is the power tower model, where thousands of heliostats (large mirrors that track the sun) focus the sun's thermal energy onto a central receiver that in turn heats molten salt to high temperatures. The heated salt is then moved to a thermal storage tank and is eventually pumped into a steam engine, which drives a standard turbine to produce electricity. Similarly, a typical coal-fired power station generates electricity by burning coal in a boiler that heats up water, which is converted into superheated steam. This steam drives a steam turbine that in turn drives a generator that produces electricity. Essentially, the CST plants can be integrated into the current power stations throughout the nation to aid in the reduction of burning of fossil fuels. Integration can either be made into feedwater heating or through supercritical steam in the power cycle [2].

1.2 Previous Studies

1.2.1 Dalvi Study

The article released by Dalvi claims that ‘there is no thermodynamic barrier to injecting solar thermal heat into Rankine-cycle plants to offset even up to 50% fossil-fuel combustion with existing technology’ [2]. To achieve this, Dalvi proposed to use solar integration in every aspect of the current Rankine-cycle coal power plants; for complete feed water heating and direct superheated steam integration into the turbines, with fuel being used to supplement this second process [2]. While this method is technically possible and fully detailed in the report, Dalvi performs this analysis with two goals in mind:

1. To motivate the government to alter current American renewable energy funding schemes to provide more substantial grants for solar-fossil fuel integration plants.
2. To illustrate that this method of emission reduction is cheaper than the alternative of carbon capture systems.

As a result of these goals, this analysis fails to take into account a fair economic evaluation when compared to the alternative of simply leaving the coal-fired power plants to operate as normal.

1.2.2 National Renewable Energy Laboratory (NREL) Paper

The NREL published a report in 2011, titled ‘Solar-Augment Potential of U.S. Fossil-Fired Power Plants’, and found that there was potential for ‘11 GWe of parabolic trough and over 21 GWe of power tower capacity’ to be introduced to America through this method [3]. The report used a ranking scheme to determine the suitability of each fossil-fired plant with 6 factors being considered; the plant’s age, capacity factor, annual average DNI at its location, amount of land available, topography of the land, and finally the solar-use efficiency. The report then goes on to determine the amount of CO_2 emissions that are avoided after the solar field is integrated into each fossil-fired power plant. The report, however, fails to accurately determine the cost of electricity produced by each solar integrated plant and instead only categorises the potential of each by metrics such a ‘fair’, ‘good’, and ‘excellent’.

This method fails to give an accurate analysis of the cost of solar heating when compared to leaving the fossil-fuel power plants to operate as normal.

1.3 Scope

Table 1.1 contains what is considered to be in and out of scope of this thesis report.

TABLE 1.1 SCOPE OF THE REPORT

In scope	Out of Scope
- Analysing the solar resource potential of the location of each coal-fired power plant in Australia - The design of various solar fields capable of integrating into Australia's coal-fired power plants - Optimising the cost of heating for the designed solar fields - Determining the resulting environmental impacts of introducing solar-coal integration in Australia	- Determining the control system required to regulate when extracted steam is needed for feedwater heating during periods of low solar irradiation - Determining the cost of the associated control system - Determining whether land is available to build a solar farm in each coal-fired power station location in Australia

1.4 Goals of the Thesis

- Explain the intermittent availability of sunlight and its application to solar thermal systems
- Determine the most feasible solar collector type for this application
- Determine the most feasible solar integration points into Australia's coal-fired power plants
- Estimate the potential space for solar input into Australia's coal-fired power plants
- Identify the costs of implementing the CST power plant solution and the resulting PPA price of electricity produced from the integrated system

- Identify the reduction in greenhouse gas emissions if the CST plant integration is implemented
- Assess the potential for solar integration of every coal-fired power plant in Australia

1.5 Outline of the Report

Chapter 2: Concentrating Solar Thermal Systems

This chapter details the various CSP collection methods available. There is a critical analysis of technologies that have been used for similar projects, and an assessment of those appropriate for this application in Australia.

Chapter 3: Coal-fired Power Plants for Analysis

This chapter outlines the schematics of the coal-fired power plants in Australia that will be used for analysis; Stanwell, Vales Point, and Yallourn Power stations. A critical analysis of solar integration input points into the coal-fired power plants is provided.

Chapter 4: Solar Resource Assessment in Australia

This chapter provides an assessment of the solar resource in Australia. An analysis of the Direct Normal Irradiance (DNI) in locations as close as possible to each coal-fired power stations in Australia has been performed. This data is essential for determining the feasibility of solar integration in each plant.

Chapter 5: Methodology

This chapter details the methodology used to attain results. Various inputs to the model will be provided, along with a clear description of the financial model that was utilised. Strengths and limitations of the model are also discussed.

Chapter 6: Results

This chapter determines the price of heating (in cents/kWh) from the integrated solar field. An analysis on the optimum solar multiple for each solar field is provided to ensure heating prices are kept to a minimum.

Chapter 7: Economic Analysis

This chapter concludes which solar collector type is the most economically viable for this application in Australia. The PPA price of electricity that is produced as a result of the solar integration system is determined. A sensitivity analysis is also conducted to ensure the validity of results and make predictions about the future costs of producing electricity from a solar-coal integrated plant.

Chapter 8: Environmental Analysis

This chapter assesses the environmental benefits of integrating solar-thermal technologies to Australia's coal-fired power plants. The amount of resulting CO2 emission reduction after integration is used as the metric for success.

Chapter 9: Conclusions

This chapter briefly states all important conclusions found in the report. In addition, an assessment on which coal-fired power plants in Australia could feasibly integrate solar-thermal power is provided.

2. Concentrating Solar Thermal Systems

2.1 Collector Types

Concentrating Solar Power (CSP) plants produce thermal energy by utilising mirrors or lenses to concentrate a large area of sunlight onto a smaller area. There is a variety of solar thermal collection techniques, however, the two main collector types are point focus systems and line focus systems [1]. The most important considerations when selecting a collector type is their operating temperature, efficiency, and associated costs. It is desirable for the collector to have high operating temperatures for use in either feedwater heating or steam integration of the current coal-fired power stations in Australia. It is important to note that for this application of integration into Australia's coal-fired power plants, no thermal storage for the solar plants is required. In a stand-alone CST system, thermal storage is required to smooth the electricity output, provide heating during periods of low or no solar radiation, and also increase the capacity factor of each power plant. To minimise expenses in this specific application, all solar thermal energy will be directly used for either feedwater heating or direct steam integration, as more coal can be burned to supplement heating during periods of low solar irradiation.

2.1.1 Point Focus Systems

2.1.1.1 Power Tower

One of the most common large-scale CSP technologies is the power tower system. This system consists of an array of ground-mounted flat mirrors known as heliostats. The heliostats are angled to reflect the sun's thermal energy onto a single solar receiver positioned atop a central tower. Heliostats are capable of dual-axis (azimuth and elevation) tracking, and are controlled by computer models [1]. These models use information such as the time and date (used to determine the sun's position in the sky), the individual heliostat's location, and the receiver's location to adjust the mirror's angle such that all thermal energy will be reflected onto the receiver.

A Heat Transfer Fluid (HTF) is then pumped through the receiver and heated. This HTF can then be used via a heat exchanger to drive steam turbines and produce electricity. In this application, the HTF will be used via a heat exchange to either provide heating for the feedwater or produce superheated steam for direct integration into the coal-fired power plant's high pressure turbine. A common HTF currently used in these plants is molten salt consisting of a blend potassium nitrate and sodium nitrate [1]. The exact blend of salt depends on the target HTF temperature. Molten salt has a high heat capacity and is therefore capable of being held in a storage tank and pumped through the receiver when electricity generation is required. The molten salt leaves the cold storage tank and enters the receiver at 290℃ and is then heated to an operating temperature of 565℃ [2]. Temperatures of up to 1000℃ are theoretically possible as a result of the high solar concentration (up to 1000 suns) of power tower systems; however, an advancement in the HTF is required to achieve this [1]. Currently, the annual solar to electricity efficiency of power tower systems is 14-18% [1]. Power tower plants cost approximately $8000/kW installed [3]. A typical layout of a power tower CSP plant is detailed below in figure 2.1.

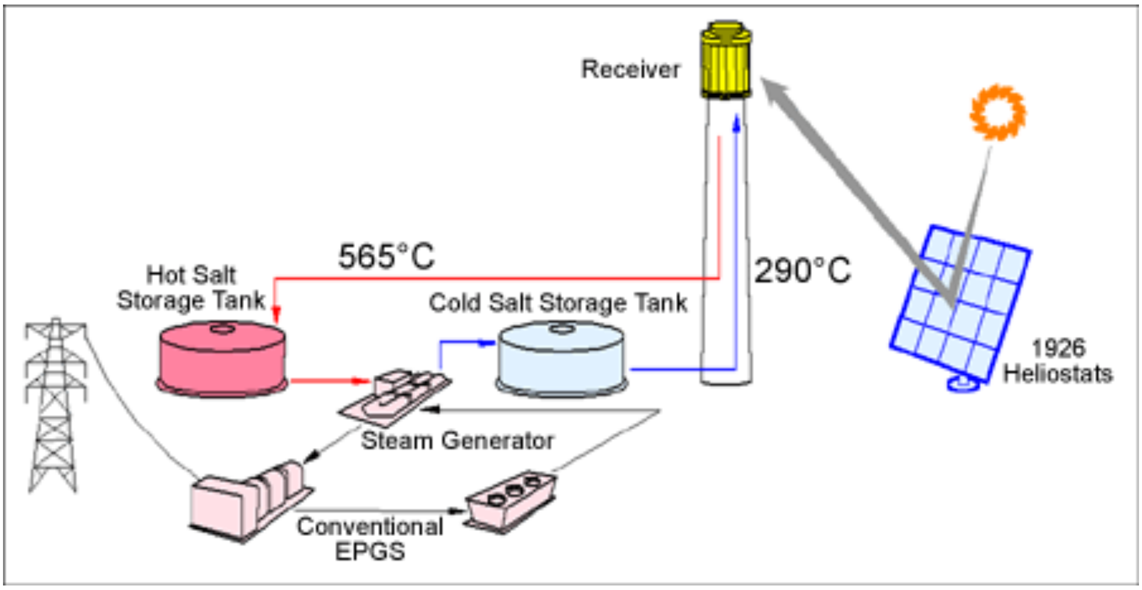

Figure 2.1 Power Tower Plant [4]

2.1.1.2 Parabolic Dish Concentrators (PDCs)

Parabolic dish concentrators are an emerging technology that use an array of mirrors attached to a large dish to concentrate the sun's thermal energy onto a receiver positioned at the dish's focal point [5]. Similar to the power tower system, parabolic dish concentrators track the sun in two axes (azimuth and elevation) throughout the day [1]. The working fluid in the receiver is heated to between 250℃ and 700℃ and is then used to power either a Stirling or Brayton engine positioned behind the receiver [2]. This method yields relatively high solar-to-electric efficiencies of up to 30% as a result of its high concentration factor of over 1300 suns [2]. Another advantage of dish concentrators is their modularity: more dishes can be built and added if required [5]. The big drawbacks of parabolic dish collectors for this application are their cost and the amount of plumbing required to connect each PDC together to provide the required amount of heat for the coal-fired power plant. This technology is more expensive per unit energy to produce when compared to all other CSP systems, largely due to the engine inbuilt within the receiver. On average, these systems cost $11000/kw to construct [3]. The layout of a PDC is detailed below in figure 2.2.

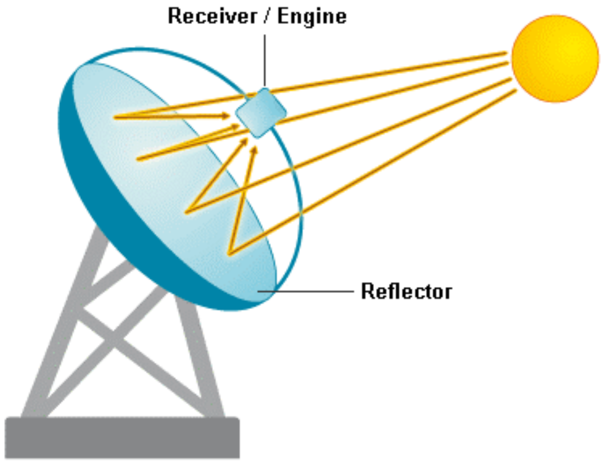

Figure 2.2 Parabolic Dish Collector [5]

2.1.2 Line Focus Systems

2.1.2.1 Parabolic trough Concentrator (PTC)

The most common CSP technology used today is the parabolic trough concentrator. This system contains arrays of parabolic mirrors that concentrate sunlight onto a receiver tube positioned at the focal line of the trough. The HTF is pumped through the tube and heated. The HTF can then be used through a heat exchanger to power a steam turbine, or in this application to heat feedwater in the coal-fired power plant. PTCs use a simple single axis tracking design which reduces its capital cost to a competitive price of $6000/kW installed with no storage, and $7000/kW with storage [2]. Furthermore, PTCs have a concentration factor of 70-80 suns resulting in operating temperatures between 350-500°C, however, thermal oil is commonly used as the HTF which limits the operating temperature to 390°C [2, 1]. Finally, PTCs have an annual solar-to-electric efficiency of 10-16% [2]. Figure 2.3 details a PTC plant setup with thermal storage integration.

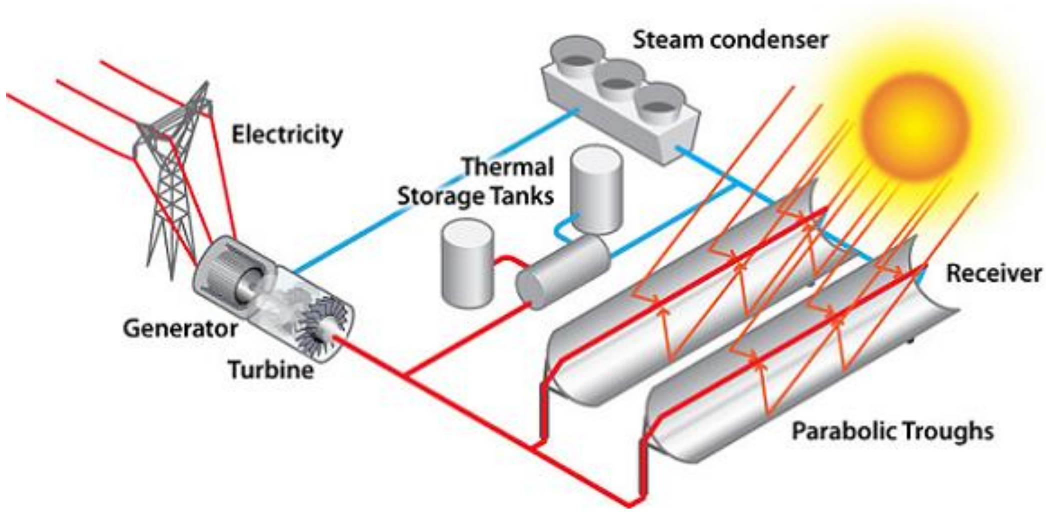

Figure 2.3 Parabolic Trough Concentrator [6]

2.1.2.2 Linear Fresnel Reflector (LFR)

Linear Fresnel Reflectors are similar to PTCs, however, they use flat mirrors to track the sun and focus its thermal energy upwards onto stationary receivers. Again, HTF is pumped through the receiver and heated, which can then be used through a heat exchanger to power a steam cycle. As a result of its simplified design, LFRs only achieve a concentration factor of 60 suns resulting in operating temperatures between 150-390°C [2]. As a result of their low operating temperatures, LFR are only useful for feedwater heating in this application as they are not capable of reaching the temperatures required for direct steam integration. The main advantage of LFRs are their low capital cost of $5000/kW installed [7]. Figure 2.4 details a LFR plant setup.

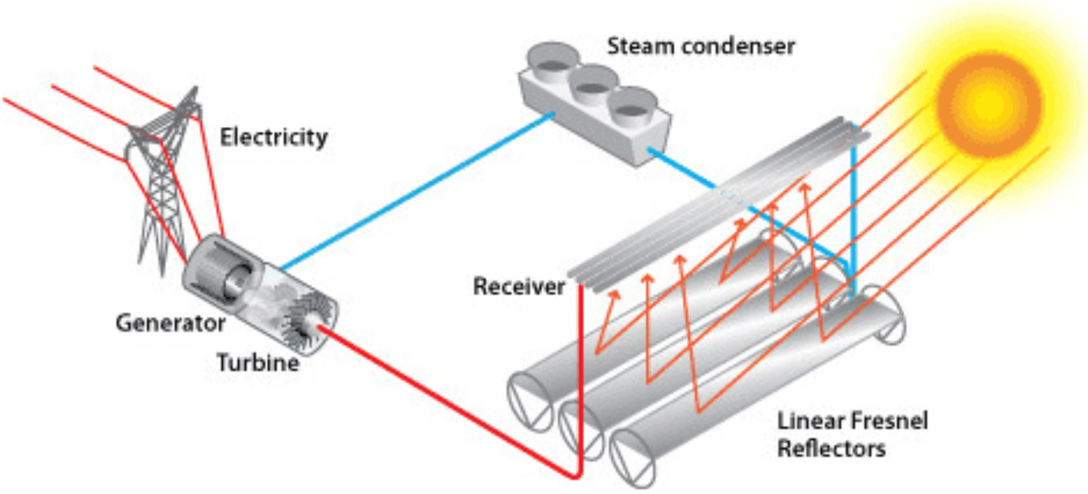

Figure 2.4 Linear Fresnel Reflector [6]

2.2 Comparison

A comparison of CSP technologies has been provided below in table 2.1. It is also important to compare the operation temperature of each CSP technology with the operation temperature of a standard coal-fired power plant as they are required to overlap for the CSP integration to work. Feedwater heating in coal-fired power stations occur in the range of 90°C to 460°C, whereas direct superheated steam integration occur in the range of 500°C to 540°C [8].

TABLE 2.1 CSP TECHNOLOGY COMPARISON [2]

Metric	Parabolic Trough	Power Tower	Linear Fresnel	Parabolic Dish
Typical capacity (MW)	10-300	10-200	10-200	0.01-0.025
Maturity of technology	Commercially proven	Pilot commercial projects	Pilot projects	Demonstration projects
Technology development risk	Low	Medium	Medium	Medium
Operating temperature (°C) **Coal-Fired Power Plant Feedwater heating: 90°C to 460°C,** **Direct Steam Integration: 500°C to 540°C**	200-500 (useful for feedwater heating)	250-565 (useful for both feedwater heating and direct steam integration)	390 (effective for feedwater heating)	550-750 (not useful for either)
Plant peak efficiency (%)	14-20	23-35	18	30
Annual solar-to-electricity efficiency (net) (%)	11-16	7-20	13	12-25
Collector concentration	70-80 suns	>1 000 suns	>60 suns (depends on secondary reflector)	>1 300 suns
Receiver/absorber	Absorber attached to collector, moves with	External surface or cavity receiver, fixed	Fixed absorber, no evacuation	Absorber attached to collector,

Metric	Parabolic Trough	Power Tower	Linear Fresnel	Parabolic Dish
	collector, complex design		secondary reflector	moves with collector
Cost ($AUD/kW installed)	6000 (no storage) 7000 (storage) [2]	8000 [2]	5000 [7]	11000 [3]
Cycle	Superheated Rankine steam cycle	Superheated Rankine steam cycle	Saturated Rankine steam cycle	Stirling/Brayton
Steam conditions (℃/bar)	(380 to 540)/100	540/(100 to 160)	260/50	N/A
Maximum slope of solar field (%)	<1-2	<2-4	<4	10% or more
Water requirement (m^3/MWh)	3 (wet cooling) 0.3 (dry cooling)	2-3(wet cooling) 0.25(dry cooling)	3 (wet cooling) 0.2 (dry cooling)	0.05-0.1 (mirror washing)
Suitability for air cooling	Low to good	Good	Low	Best
Viable for Coal-Fired Plant integration	Yes	Yes	Yes, for feed water heating	Not currently

Clearly, the most viable options for CSP integration to Australia's coal-fired power plants are the power tower and parabolic trough collector systems. Both technologies have high solar concentration and operating temperatures in conjunction with relatively low capital costs. The power tower system has operating temperatures that would be useful for both feedwater heating and direct steam integration to Australia's coal-fired power plants. In comparison, the PTC systems will only be useful for feedwater heating. The Linear Fresnel Reflector system attains reasonably low operating temperatures with its upper temperature limit falling short of the upper bound on feedwater heating. In contrast, parabolic dish collectors have very high operating temperatures, however, this temperature is used directly into a Stirling/Brayton engine. Large heat losses would result if the HTF from the PDC receiver was transported to a heat exchanger to produce steam for integration with coal-fired plants, especially in a utility-scale plant. Furthermore, the capital cost of PDCs are considerably higher than other technologies and they have not been commercially demonstrated.

2.3 Current Systems

The idea of such solar-aided fossil-fuel power plants has been investigated for some time and such plants are shown to be significantly more cost effective than the conventionally deployed solar-thermal plants. These integration methods have shown to reduce the cost of solar thermal power by 30-50% [9]. Notable plants executing this strategy are detailed below in table 2.2.

TABLE 2.2 CURRENT SOLAR-FOSSIL INTEGRATION SYSTEMS [9]

Power Plant	Fossil Fuel Type	Location	Nameplate Capacity (MW)	CSP Technology Utilised	Percent Integration (%)
Martin Next Generation Solar Energy Centre	Natural Gas	Florida, USA	1150	Parabolic Trough	2
ISCC Kuraymat	Natural Gas	Egypt	140	Parabolic Trough	15
ISCC Hassi R'Mel	Natural Gas	Algeria	150	Parabolic Trough	17
Kogan Creek*	Coal	Australia	750	Linear Fresnel	5.8

*The Kogan Creek Solar Boost project was discontinued for cost reasons.

Unfortunately, to this date, many of these projects have underperformed on their projected modellings of both capital cost and energy output. The Martin Next Generation Solar Energy Centre (MNGSEC) began construction in 2008 on the 75MW array of 190,000 mirror parabolic troughs and was completed in 2010 at a capital cost of over $476 million [12]. In 2012, the solar plant contributed to the production of 89GWh of energy, however, this fell short by 42% of its projected modelling when approved. In the following years this energy output value from the solar farm has been more favourable; in 2014 the plant operated at 99% of its projected modelling [12]. The plant is still considered a success, and the cost of electricity production from the solar farm is nearly 30% cheaper than a stand-alone PTC system in the same area (Florida) could produce, based on DNI figures [12].

3. Coal-Fired Power Plants for Analysis

3.1 Overview

Three of Australia's coal-fired power plants will be used for analysis: Stanwell Power Station, Vales Point Power Station, and Yallourn Power Station. The plant block diagrams for each station can be found in sections 3.3, 3.4, and 3.5 of this report, respectively. Table 3.1 details the location, capacity, and type of coal used in each station.

TABLE 3.1 POWER STATIONS FOR ANALYSIS

Power Station	Location	Capacity (MW)	Type of Coal Used
Stanwell	QLD	1445	Black
Vales Point	NSW	1320	Black
Yallourn	VIC	1480	Brown

3.2 Integration Points

There are two types of solar integration points into the coal-fired power stations: feedwater heating and direct steam integration. Each method has been analysed to determine which is most feasible for application in Australia.

3.2.1 Feedwater Heating

In a standard coal-fired power plant steam is extracted from the turbines to provide feedwater heating for the boiler. In the proposed integrated system, molten salt carrying solar energy, which is produced in the CSP plant, replaces the extraction steam to heat the feedwater and the steam thus saved can continue to do work (as detailed in figure 3.1). As the solar heat does not enter the turbine, the efficiency of solar to power is not limited by the temperature of the solar heat [10].

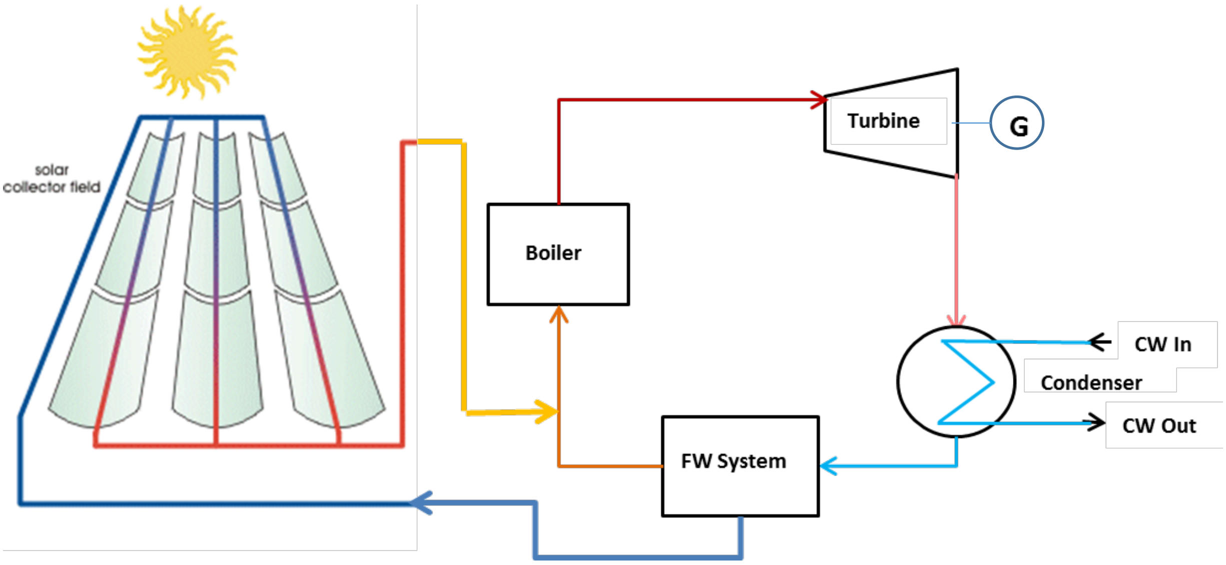

Figure 3.1 Feedwater Heating [10]

3.2.2 Direct Steam Integration

This method is achieved when high pressure feed water is taken through the solar thermal plant to generate steam, which is then fed to the high pressure (HP) steam turbine inlet to directly produce electricity (as detailed in figure 3.2). This method of integration requires much higher working temperatures resulting in the need for a larger and far more expensive CST system. It is also easier and more efficient to build a turbine directly for this large-scale CST plant and have it optimised to meet its requirements rather than completing integration into existing conventional systems. This is especially true as the turbine costs are a fraction of the cost to build a large scale power plant [10].

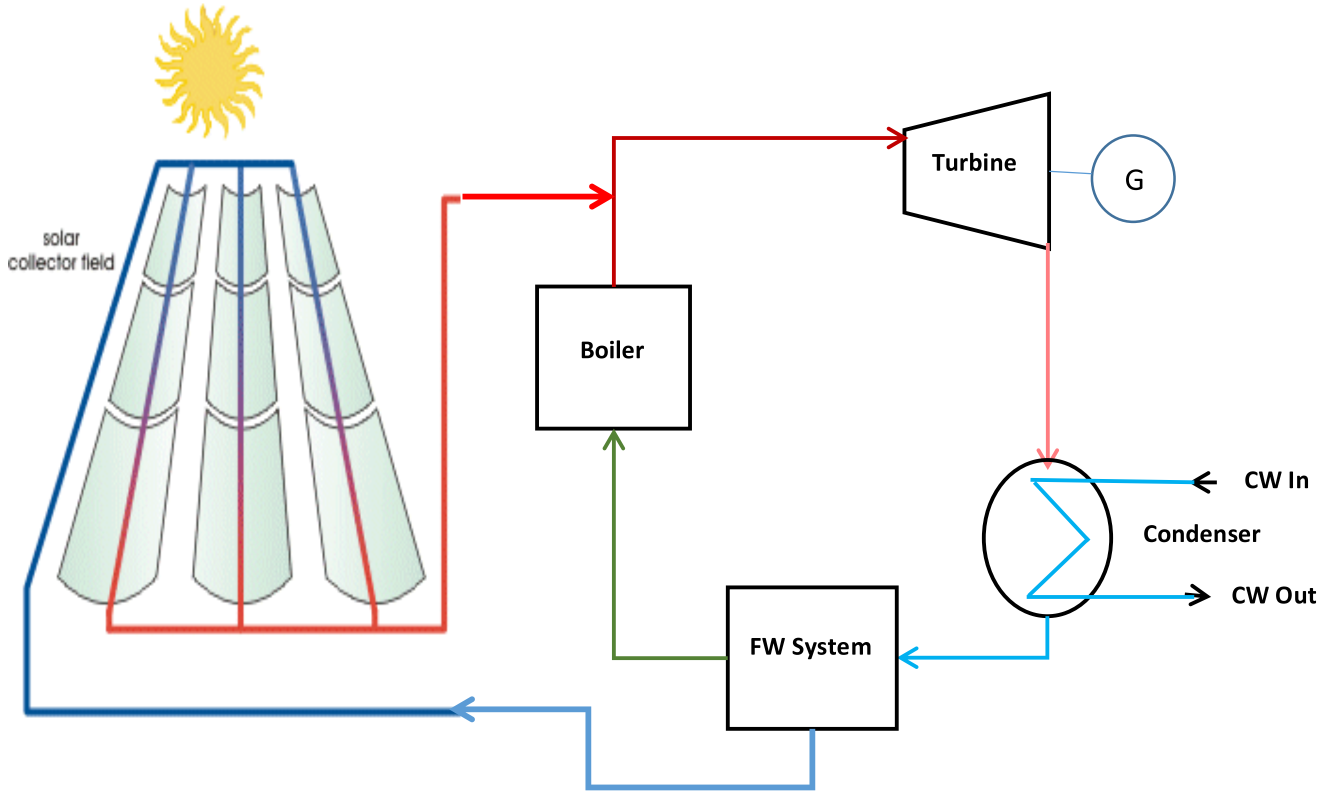

Figure 3.2 Direct Steam Integration [10]

3.2.3 Integration for Australia's Coal-Fired Power Plants

Feedwater heating was determined to be the most effective and economic way to integrate CSP into Australia's coal fired power plants. As discussed in section 2 of this report, all CSP collectors were compared and the PTC and power tower systems were determined to be the most appropriate for this application as a result of their high solar concentration and operating temperatures in conjunction with relatively low capital costs. Both systems have excellent temperature ranges that encompass the range of steam temperatures used for feedwater heating in conventional coal-fired power station (90-460°C).

Figure 3.3 details a simplified version of the feedwater heating section in a conventional coal-fired power plant. The feedwater input points have been labelled 1 through 7 starting at the feedwater input closest to the boiler. This is the labelling that will be used for the remainder of the report. Feedwater inputs 1 and 2 are heated by high pressure, temperature, and mass flow rate extraction steam that as a result, have high enthalpy values [12]. Moving along from inputs 3 to 7, the temperature, pressure, and mass flow rate of the steam used to heat each input gradually reduces, resulting in lower enthalpy steam. Steam that has higher enthalpy and mass flow rate values can produce greater work when passing through a turbine, as turbine work (W) can be calculated as:

$$W = m_s(h_i - h_o) \qquad (1)$$

Where; m_s is the mass flow rate of steam, and h_i and h_o are the input and output enthalpies of the steam, respectively.

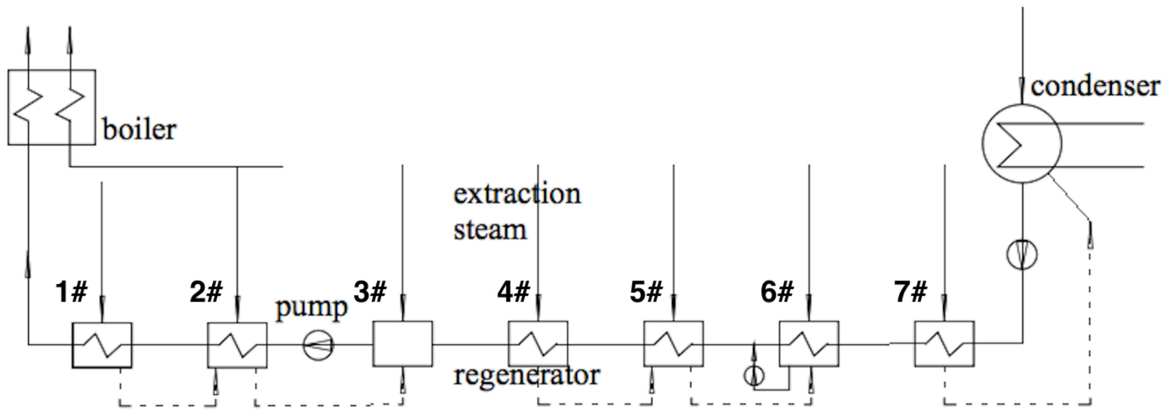

Figure 3.3 Simplified Coal-Fired Power Plant Feedwater Integration Section

A report by Hongjuan [12] in 2012 titled 'Solar-Coal Hybrid Thermal Power Generation', explains that as a result of these factors, only feedwater inputs 1 and 2 are economically feasible to use solar fields for their heating. The report goes on to explain that each feedwater input requires its own solar field to be optimised and have the output fluid temperature of the field be equal to the extraction steam temperature that would otherwise be utilised [12]. As a result of this, the remainder of this report will focus on analysis of solar fields for both 'feedwater input 1' and 'feedwater input 2'.

3.3 Stanwell Power Station Block Diagram

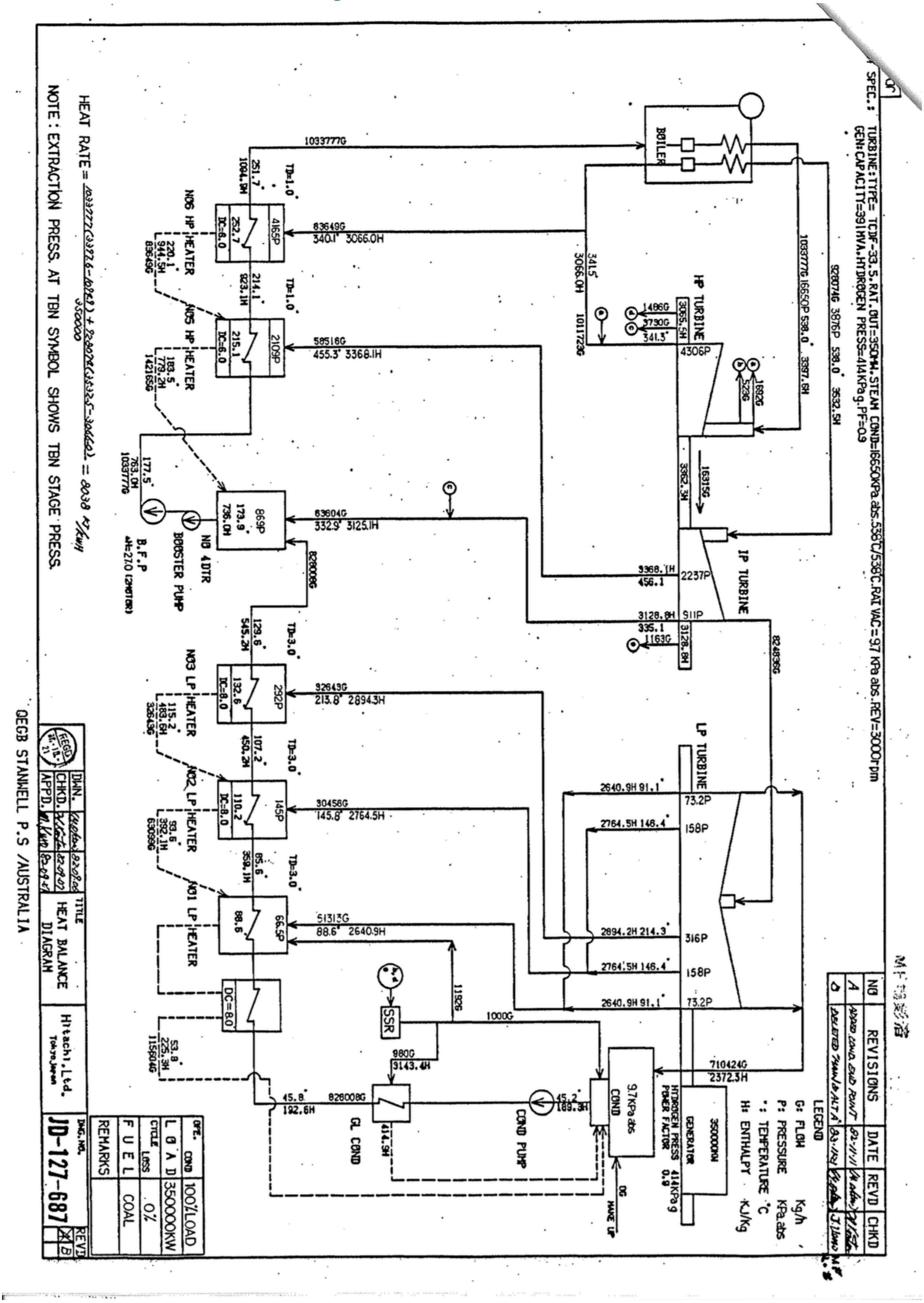

3.4 Vales Point Power Station Block Diagram

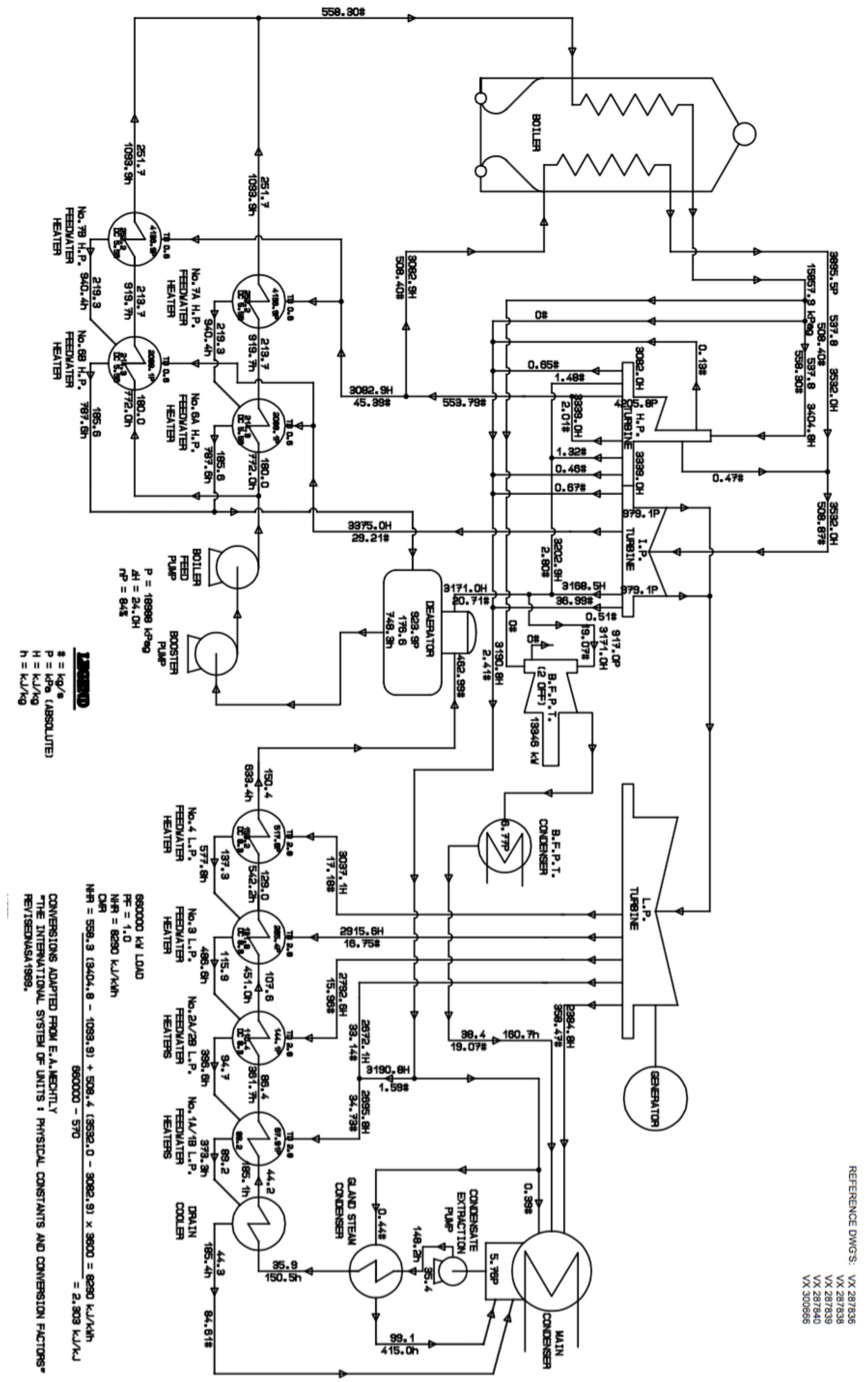

3.5 Yallourn Power Station Block Diagram

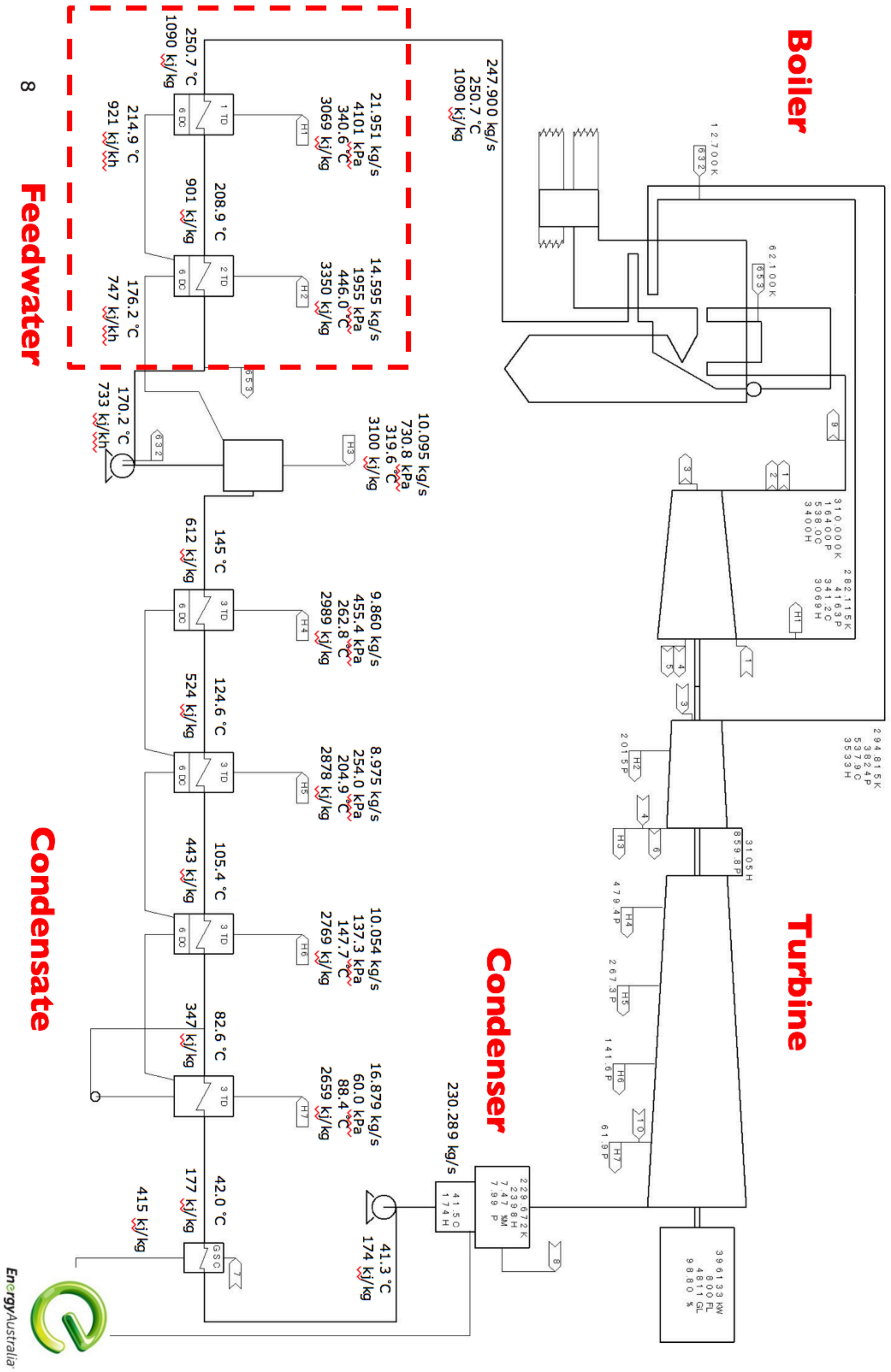

4. Solar Resource Assessment in Australia

4.1 Solar Radiation Theory

The source of energy used by CSP plants is the sun. Solar radiation is radiant energy emitted by the sun in the form of electromagnetic vibrations at varying frequencies [11]. Low frequency waves produce UV light, whereas high frequency waves produce infrared light, with visible light situated in-between. The terrestrial solar spectrum details the amount of irradiance versus the frequency of a light wavelength (figure 4.1). The term *irradiance* refers to the energy flux of light and has units $\frac{W}{m^2}$ [11].

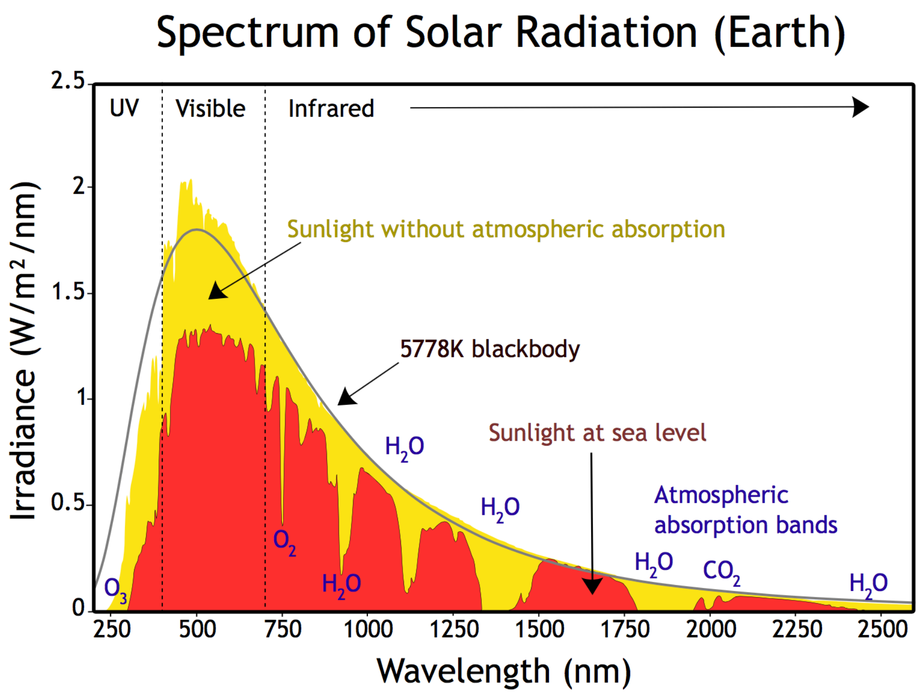

Figure 4.1 Solar Spectrum [11]

The irradiance falling on the Earth's surface changes by approximately 6.66% annually as a result of the variation in the distance between the earth and the sun [11]. Furthermore, solar activity can result in irradiance changes of up to 1% [11]. Irradiance received on the Earth's surface is also highly susceptible to local meteorological conditions such as cloud cover, and as such, it is difficult to forecast. As a result of this, monthly average profiles are used to provide area-specific forecasts. Reliable irradiance data is essential to the feasibility analysis of a proposed solar power project.

4.1.1 Components of Radiation

The spectrum of solar radiation has several components. As detailed in figure 4.2, a portion of light emitted by the sun is lost when it is absorbed or scattered by the atmosphere or reflected off interfering bodies such as clouds. The total amount of global radiation consists of the light that reaches the ground and is split into two components: direct and indirect radiation [12].

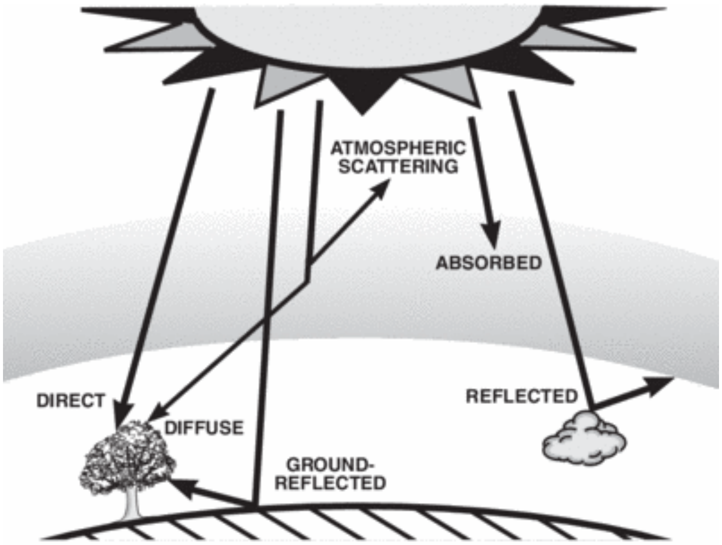

Figure 4.2 Solar Radiation Components [12]

4.1.1.1 Direct Radiation

Direct radiation, also referred to as Direct Normal Irradiance (DNI), is received straight from the sun, unobstructed by the atmosphere or clouds. DNI is received on a plane perpendicular to the beam and is usually measured using a pyrheliometer, which is mounted on a solar tracker [13]. It represents the highest level of energy flux available at a given time. Concentrating solar thermal systems only utilise DNI as a power source, which is why solar tracking is so important to this technology (as the panels need to be perpendicular to direct sunlight throughout the day to achieve maximum efficiency).

4.1.1.2 Indirect Radiation

Indirect or diffuse radiation is solar radiation that has either been scattered by the atmosphere or reflected back to a surface from the ground. Diffuse solar irradiance can be thought of as all energy incident on a plane that is shaded from the direct light of the sun [13].

4.1.1.3 Global Radiation

Global radiation is the sum of the direct and indirect radiation, and is a measure of the total incoming rate of energy. This relationship can be used for both instantaneous values of flux $\left(\frac{W}{m^2}\right)$ and time-averaged values $\left(\frac{MJ}{m^2 day}\right)$ [12]. A value for global radiation can be attained by summing diffuse radiation and the horizontal component of direct radiation as detailed in equation 2 [11].

$$Global\ Radiation = DNI \times cos(z) + Diffuse\ Radiation \qquad (2)$$

Where z is the zenith angle of the sun as detailed in figure 4.3.

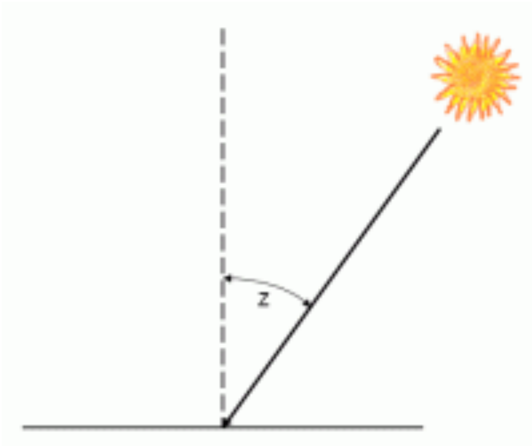

FIGURE 4.3 ZENITH ANGLE [14]

4.2 Measurement and Estimation of Solar Radiation

The accurate measurement of solar radiation is highly important to assessing the potential of a CSP project in a given area. Mirrors and concentrating optics utilised in CSP technologies are only capable of focussing DNI. Therefore, only technologies that measure DNI values are useful to be appraised.

4.2.1 Pyrheliometer

A pyrheliometer is the main instrument currently used to measure DNI. Light (between 200 and 4000nm in wavelength) enters the device through a glass window and is directed onto a thermopile, which converts thermal energy into electrical energy [15]. The electrical signal is then converted to measure $\frac{W}{m^2}$ using a formula. The pyrheliometer is connected to a solar tracking device (as it only has a field of view of approximately 5 degrees) and receives radiation directly from the orb of the sun, while blocking any diffuse radiation. Figure 4.4 details pyrheliometer attached to a solar tracking device.

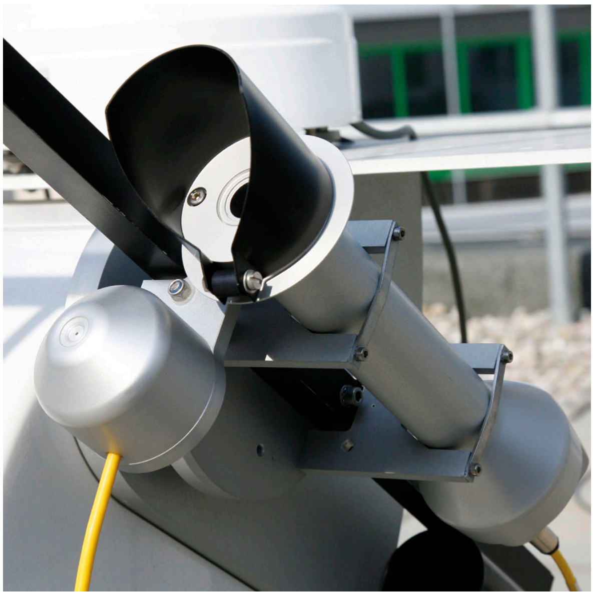

Figure 4.4 Pyrheliometer [13]

4.3 Australia's DNI Distribution

Australia has one of the highest solar resource potential when compared to the world, which can be explained by its proximity to the equator and weather patterns [16]. The DNI distribution in Australia is detailed in figure 4.5.

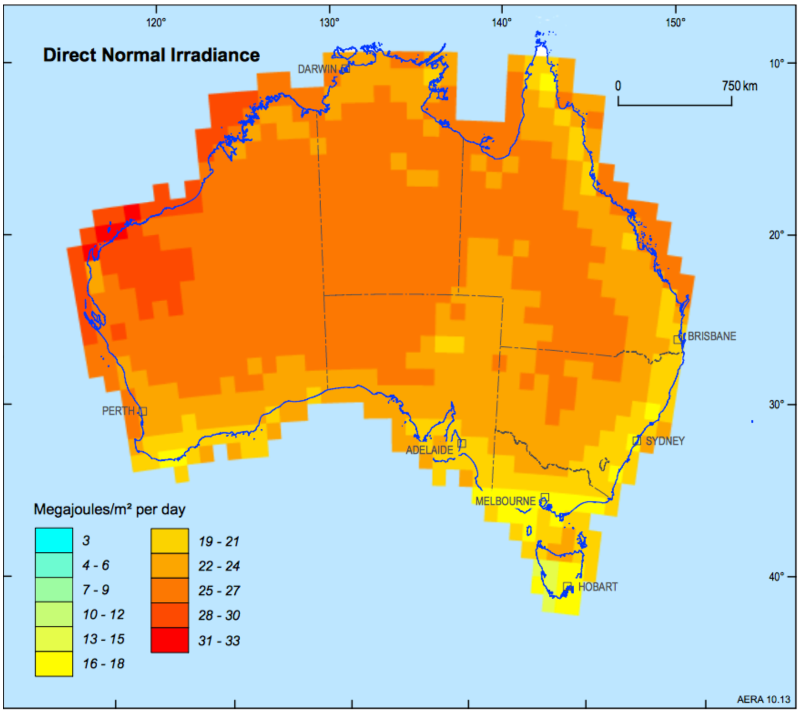

Figure 4.5 Australia's DNI distribution [16]

An assessment of the DNI location data for each coal-fired power plant is essential to analysing the feasibility of each project. Unfortunately, the open-source DNI data for Australia is limited, with only minimal resources available at this time. As such, DNI distribution will be broken down state by state, and the difference in distance and direction between the coal-fired plants and data will be noted. The direction will either be highlighted green to indicate that the location is likely to have higher irradiation than the given resource, or red, to indicate the opposite. As previously mentioned, within these annual DNI figures, there will be days of irregularly low solar irradiance as a result of weather systems. Cloud and fog cover for extended periods of time, which can occur during the Australian wet season, will significantly reduce the amount of DNI recorded. As such the annual mean DNI distribution in $W/_{m^2}$ will be provided for each solar resource, and will be used to determine the each location's solar potential.

4.3.1 Queensland

Table 4.1 details the coal-fired power stations in Queensland along with their max capacity (MW), closest DNI resource, distance differential and direction to that resource (km), and the solar resource's annual mean DNI value from SAM. Figure 4.6 and 4.7 represents the annual DNI distribution in Chinchilla, QLD and Longreach, QLD respectively.

TABLE 4.1 QUEENSLAND PLANT DNI ASSESSMENT [17]

Power station	Max. Capacity (MW)	Closest Resource	Difference in Distance (km)	Difference in Direction	Annual Mean DNI Value $\left(W/_{m^2}\right)$
Collinsville	190	Longreach, QLD	600	**NE towards coast**	294
Tarong North	443	Chinchilla, QLD	160	**E towards coast**	268
Callide A & B	730	Chinchilla, QLD	350	**N towards coast**	268
Kogan Creek	750	Chinchilla, QLD	25	**W Inland**	268
Millmerran	852	Chinchilla, QLD	170	**SE towards coast**	268

Power station	Max. Capacity (MW)	Closest Resource	Difference in Distance (km)	Difference in Direction	Annual Mean DNI Value $\left(W/_{m^2}\right)$
Callide C	900	Chinchilla, QLD	350	N towards coast	268
Tarong	1,400	Chinchilla, QLD	150	E towards coast	268
Stanwell	1,445	Chinchilla, QLD	460	N towards coast	268
Gladstone	1,680	Chinchilla, QLD	480	N towards coast	268

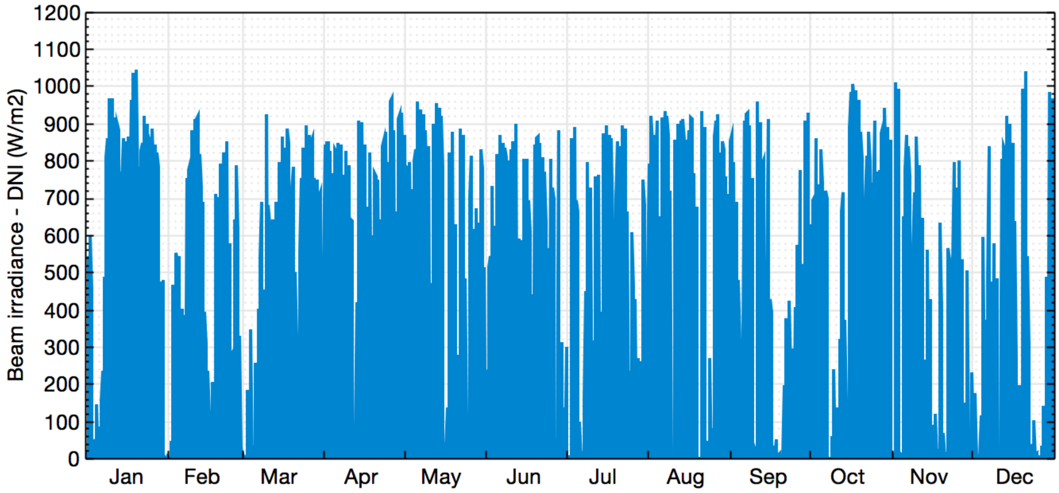

Figure 4.6 Annual DNI distribution in Chinchilla, QLD [18]

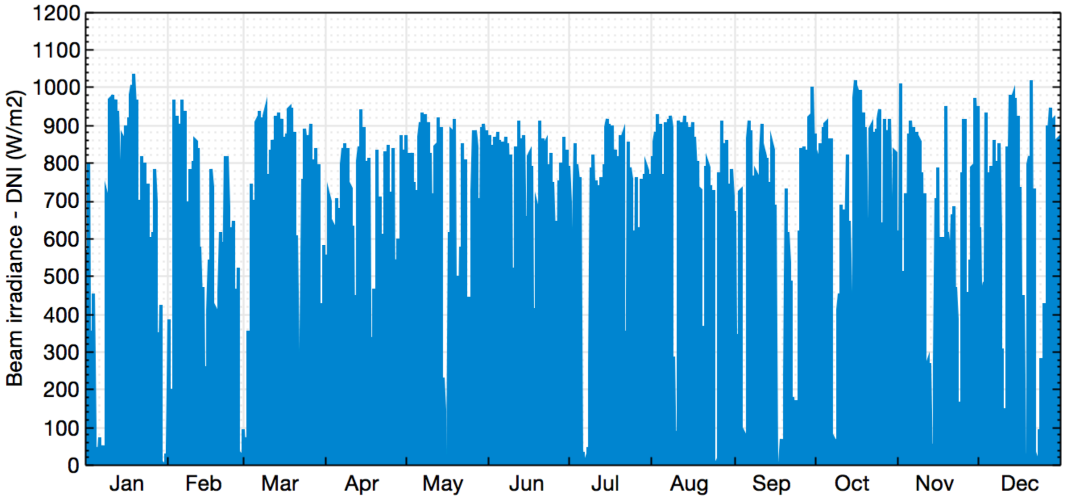

Figure 4.7 Annual DNI distribution in Longreach, QLD [18]

4.3.2 New South Wales

Table 4.2 details the coal-fired power stations in New South Wales along with their max capacity (MW), closest DNI resource, distance differential and direction to that resource (km), and the solar resource's annual mean DNI value from SAM. Figure 4.8 represents the annual DNI distribution in Sydney, NSW.

TABLE 4.2 NEW SOUTH WALES POWER PLANT DNI ASSESSMENT [17]

Power station	Max. Capacity (MW)	Closest Resource	Difference in distance (km)	Difference in Direction	Annual Mean DNI Value $\left(W/_{m^2}\right)$
Vales Point	1,320	Sydney, NSW	120	N along coast	166
Mt Piper	1,400	Sydney, NSW	160	W Inland	166
Liddell	2,000	Sydney, NSW	240	N Inland	166
Bayswater	2,640	Sydney, NSW	240	N Inland	166
Eraring	2,880	Sydney, NSW	140	N along coast	166

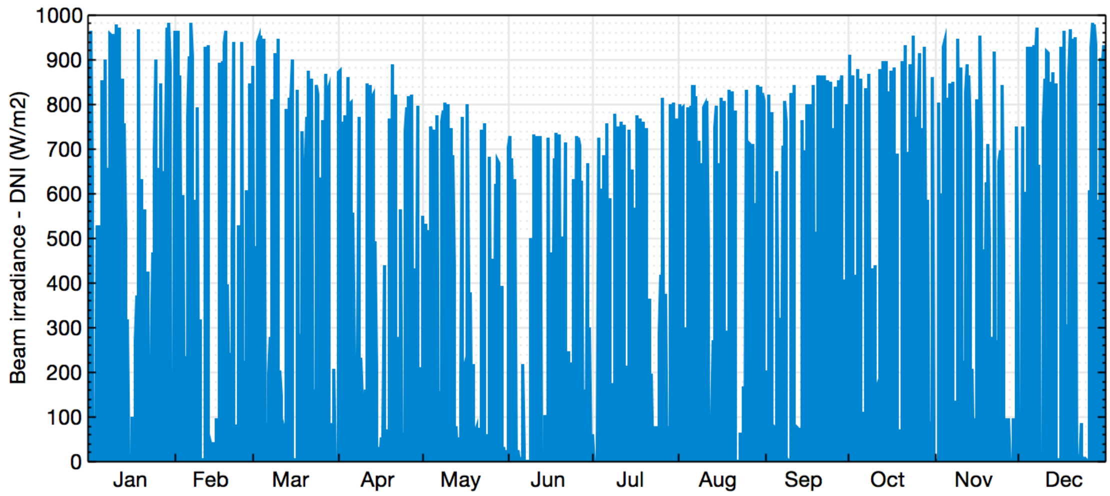

Figure 4.8 Annual DNI distribution in Sydney, NSW [18]

4.3.3 Victoria

Table 4.3 details the coal-fired power stations in Victoria along with their max capacity (MW), closest DNI resource, distance differential and direction to that resource (km), and the solar resource's annual mean DNI value from SAM. Figure 4.9 represents the annual DNI distribution in Melbourne, VIC.

TABLE 4.3 VICTORA PLANT DNI ASSESSMENT [17]

Power station	Max. Capacity (MW)	Closest Solar Resource	Difference in Distance (km)	Difference in Direction	Annual Mean DNI Value $\left(W/_{m^2}\right)$
Hazelwood	1,600	Melbourne, VIC	140	**SE towards coast**	134
Loy Yang A	2,200	Melbourne, VIC	160	**SE towards coast**	134
Loy Yang B	1,050	Melbourne, VIC	160	**SE towards coast**	134
Yallourn	1,480	Melbourne, VIC	140	**E inland**	134

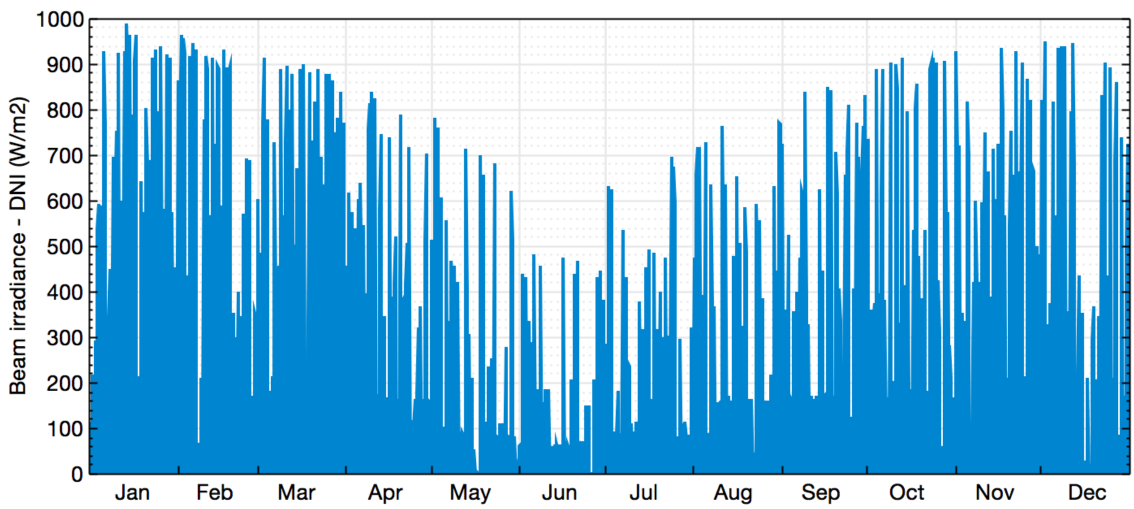

Figure 4.9 Annual DNI distribution in Melbourne, VIC [18]

4.3.4 South Australia

Table 4.4 details the coal-fired power stations in South Australia along with their max capacity (MW), closest DNI resource, distance differential and direction to that resource (km), and the solar resource's annual mean DNI value from SAM. Figure 4.10 represents the annual DNI distribution in Port Augusta, SA.

TABLE 4.4 SOUTH AUSTRALIA PLANT DNI ASSESSMENT [17]

Power station	Max. Capacity (MW)	Closest Resource	Difference in Distance (km)	Difference in Direction	Annual Mean DNI Value $\left({}^{W}/_{m^2}\right)$
Northern	520	Port Augusta, SA	9	Neutral	260
Playford B	240	Port Augusta, SA	12	Neutral	260

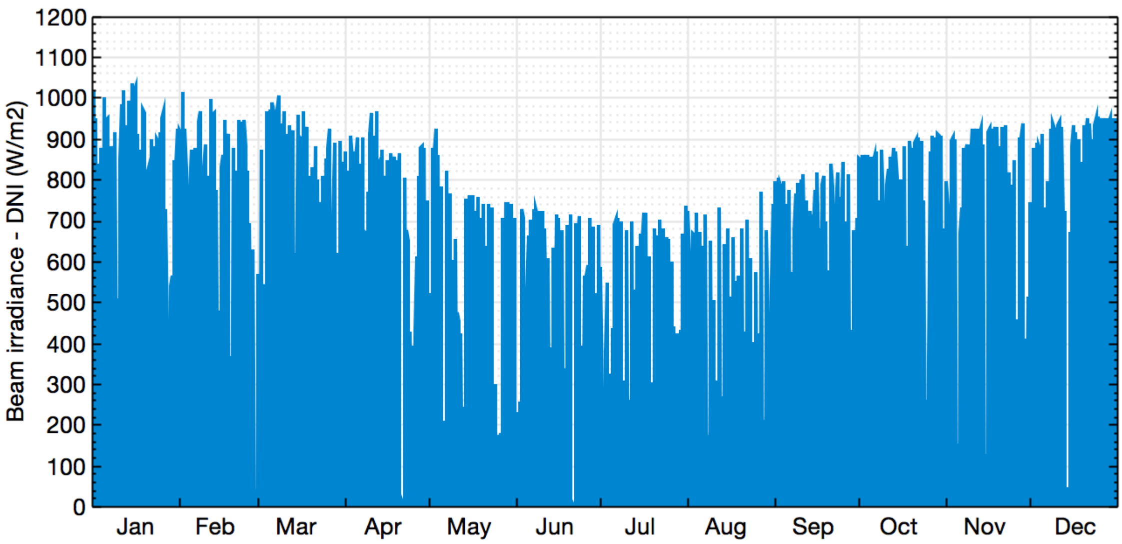

Figure 4.10 Annual DNI distribution in Port Augusta, SA [18]

4.3.5 Western Australia

Table 4.5 details the coal-fired power stations in Western Australia along with their max capacity (MW), closest DNI resource, distance differential and direction to that resource (km), and the solar resource's annual mean DNI value from SAM. Figure 4.11 represents the annual DNI distribution in Perth, WA.

TABLE 4.5 WESTERN AUSTRALIA PLANT DNI ASSESSMENT

Power station	Max. Capacity (MW)	Closest Resource	Difference in Distance (km)	Difference in Direction	Annual Mean DNI Value $\left(W/_{m^2}\right)$
Worsley Alumina Power Station	107	Perth, WA	190	S along coast	222
Collie	300	Perth, WA	210	S along coast	222
Bluewaters	416	Perth, WA	200	S along coast	222
Kwinana	640	Perth, WA	35	S along coast	222
Muja	854	Perth, WA	220	S along coast	222

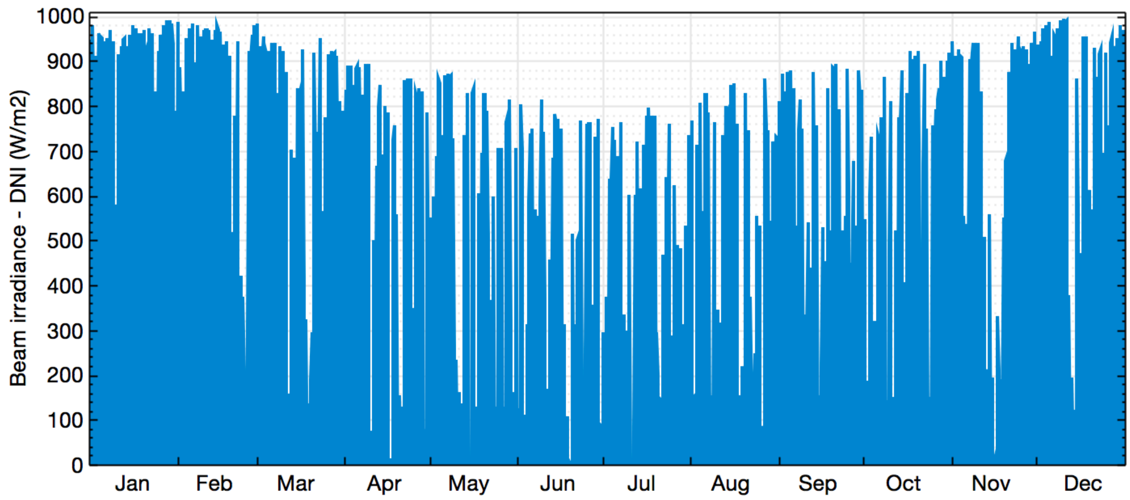

Figure 4.11 Annual DNI distribution in Perth WA [18]

5. Methodology

5.1 System Advisory Model

The performance of the integrated system was analysed using the System Advisory Model (SAM), a CSP analysis tool produced by the National Renewable Energy Laboratory (NREL). SAM makes 'performance predictions and cost of energy estimates for grid-connected power projects based on installation and operating costs and system design parameters that you specify as inputs to the model' [19]. SAM utlisies the annual DNI data for a given location to both size and provide annual cost and capacity data for a solar power plant. Once a model is produced, SAM allows for parametric analysis of every variable that has been entered, allowing for efficient optimization of the system.

The SAM input tools differ for parabolic trough installations and power tower models, and as such, step by step methods can be found for each in sections 5.1.2 and 5.1.3 of this report, respectively.

5.1.1 Power Calculations

One of the most important input metrics to SAM is the gross power output of the desired solar power plant. In this model, the solar field is required to produce enough steam to replace the amount of turbine extracted steam at each feedwater input. Therefore, the amount of heat the solar plant needs to produce is equal to the amount of heat provided from the extraction steam. The amount of heat provided by the extraction steam can be calculated from thermodynamic principles.

$$m_s = \frac{q}{h_e} \qquad (3)$$

Where; m_s(kg/s) is the mass flow rate of the steam, q (kJ/s) is the mean heat transfer rate, and h_e (kJ/kg) is the evaporation heat of steam at a given pressure. The values for m_s and h_e can be read and calculated from the coal-fired power plant diagrams found in section 3.3, 3.4, and 3.5 of this report.

As previously mentioned, SAM requires the 'gross power output' as an input to the model and not 'gross heat output (q)' of the solar field. In addition, SAM provides simulation outputs in terms of electricity energy produced instead of heat energy produced as it assumes the solar field is connected to a power cycle (turbine and generator), however, this is not the case is this model. The solar field in this model is simply being used to facilitate the heating of steam in the coal-fired power plant, and not to directly produce electricity. To overcome this issue, an arbitrary cycle conversion efficiency value 0.5 is inputted to the model. This tricks SAM into thinking the solar field is connected to a turbine that is 50% efficient, which despite being higher than standard turbines, it still allows the simulations to run without error. This means that the below equation holds true.

$$PowerOutput_{gross} = HeatOutput_{gross} \times 0.5 \qquad (4)$$

Table 5.1 below details the 'gross power output' required from each feedwater heating point from each coal-fired power station being used for analysis. The 'gross power outputs' listed in the final column of table 5.1, were then used as inputs to SAM to size each solar field.

TABLE 5.1 GROSS POWER OUTPUT CALCULATIONS

Power Station	Feedwater Input	Mass Flow Rate of Steam (m_s – kg/s)	Pressure of Steam (kPa)	Evaporation Heat of Steam (h_e – kJ/kg)	Heat Provided by Steam (q – MW)	Gross Power Output for SAM (MW)
Stanwell	1	23.235	4165	1704	39.6	**19.8**
	2	16.254	2109	1878	30.5	**15.3**
Vales Point	1	45.39	4196	1700	77.2	**38.6**
	2	29.21	2098	1878	54.8	**27.4**
Yallourn	1	21.951	4101	1708	37.5	**18.8**
	2	14.595	1955	1896	27.7	**13.8**

5.1.2 Parabolic Trough SAM Inputs

The input parameters for parabolic trough systems to the SAM are broken down into 13 different sections. Table 5.2 lists each section, gives a brief overview of its importance, and states the important input parameters that were used for this model.

TABLE 5.2 PARABOLIC TROUGH SAM INPUT PARAMETERS

SAM Section	Overview and Inputs
Location and Resource	SAM provides annual weather data for any location within its database. This data is then inputted to the model and provides the resource for cost outputs and sizing solar field calculations. Stanwell: Chinchilla Vales Point: Sydney Yallourn: Melbourne
Solar Field	In this section is it possible to alter various parameters to do with the parabolic trough and heat transfer system design. *Solar Multiple*: Optimised in parametric analysis *Design Point Irradiation*: This is considered to be the DNI level that the solar farm is designed towards. If this DNI level was maintained throughout the year, the solar plant with a solar multiple of 1 would operate at 100% capacity. SAM advises this 'design point irradiation' to be the DNI that occurs at 12 noon on the equinox (September 23rd in Australia) Stanwell = 950 W/m^2 Vales Point = 850 W/m^2 Yallourn = 800 W/m^2 *Heat Transfer Fluid*: HiTec Solar Salt *Design Loop inlet temp*: 293°C *Design Loop outlet temp*: Based on each coal-fired power stations temperature of steam at feedwater points 1 and 2. Stanwell 1 = 380.1°C Stanwell 2 = 495.3°C Vales Point 1 = 380.6°C Vales Point 2 = 486°C Yallourn 1 = 381°C Yallourn 2 = 490.3°C Note: *these temperatures are all 40°C higher than those read of the plant diagrams to account for heat exchanger losses* Non-solar field land area multiplier = 1.3 For all other input parameters refer to appendix A.1.
Collectors	In this section it is possible to choose the solar collector type and SAM details its resulting parameters.

	Solar Collector Type: Solargenix SGX-1 For the resulting geometry and parameters refer to appendix A.2.
Receivers	In this section it is possible to choose the solar receiver and SAM details its resulting parameters. Solar Receiver Type: Schott PTR80 For the resulting parameters refer to appendix A.3.
Power Cycle	In this section the gross power output of the desired power plant is specified. *Design Gross Power Output*: refer to table 5.1 *Estimated Gross to Net Conversion Factor*: 1 *Rated Cycle Efficiency*: 0.5 For a detailed look at the power cycle parameters refer to appendix A.4.
Thermal Storage	In this section the thermal storage hours and system can be specified. For this model, no storage is required and therefore, the amount of storage hours is set to zero.
Parasitics	In this section various parasitic parameters can be specified. Piping Thermal Loss Coefficient: $0.45\,\frac{W}{m^2K}$ Tracking Power: $125\ \frac{W}{sca}$
System Costs	In this section it is possible to specify both direct and indirect capital costs along with operational and maintenance costs. These figures were obtained from the Austella (2014) 'Australian Guide to SAM for Concentrating Solar Power' [20]. A sensitivity analysis is performed on these figures in section 7 of this report. *Site Improvements*: $30\,\frac{\$}{m^2}$ *Solar Field*: $170\,\frac{\$}{m^2}$ *HTF System*: $70\,\frac{\$}{m^2}$ *EPC and Owner Cost*: 11% of direct capital cost *Total Land Cost*: $10000\,\frac{\$}{acre}$

	Note: It is assumed that no adjacent land is owned by the coal-fired power station companies. If the land was owned, it would lower capital costs. *Fixed O&M by Capacity*: $66\frac{\$}{kW-yr}$ *Variable O&M by Generation*: $4\frac{\$}{MWh}$
Lifetime	This section provides the means to incorporate a system performance degradation rate, which reduces the energy production (in kWh) by a certain percent each year. For the purposes of this modelling the degradation rate has been left at zero percent.
Financial Parameters	See section 5.2 of the report.
Time of Delivery Factors	This section alters the PPA price of the electricity produced based on the time of day and month of the year is it produced in. Uniform dispatch (constant PPA price throughout the year and throughout each day) was used for this analysis.
Incentives	No incentives were used in this modelling to ensure fair economic analysis was achieved.
Depreciation	See section 5.2 of the report.

5.1.3 Power Tower SAM Inputs

The inputs parameters for power tower systems to the SAM are broken down into 13 different sections. Table 5.2 lists each section, gives a brief overview of its importance, and states the important input parameters that were used for this model.

TABLE 5.3 POWER TOWER SAM INPUT PARAMETERS

SAM Section	Overview and Inputs
Location and Resource	Refer to table 5.1
System Design	In this section is it possible to alter various parameters to do with the power tower and heat transfer system design. *Design Point Irradiation*: This is considered to be the DNI level that the solar farm is designed towards. If this DNI level was maintained throughout the year, the solar plant with a solar multiple of 1 would operate at 100% capacity. SAM advises this ‘design point irradiation’ to be

	the DNI that occurs at 12 noon on the equinox (September 23rd in Australia) Stanwell = 950 W/m^2 Vales Point = 850 W/m^2 Yallourn = 800 W/m^2 *HTF Cold Temperature*: 293℃ *HTF Hot Temperature*: Based on each coal-fired power stations temperature of steam at feedwater points 1 and 2. Stanwell 1 = 380.1℃ Stanwell 2 = 495.3℃ Vales Point 1 = 380.6℃ Vales Point 2 = 486℃ Yallourn 1 = 381℃ Yallourn 2 = 490.3℃ Note: *these temperatures are all 40*℃ *higher than those read of the plant diagrams to account for heat exchanger losses* *Thermal Storage Hours*: 0 hours *Design Gross Power Output*: refer to table 5.1 *Estimated Gross to Net Conversion Factor*: 1 *Rated Cycle Efficiency*: 0.5
Heliostat Field	In this section it is possible to optimise the heliostat field design, including the geometry of the heliostat. SAM includes a tool that allows the user to 'optimise heliostat design', which calculates the heliostat geometry and number of heliostats required to have maximise power output while minimising cost. This tool was used before each simulation was run to ensure optimal parameters were used. For the resulting geometry and parameters of the heliostat field refer to appendix A.5.
Tower and Receiver	In this section, SAM uses the system design parameters such as; solar multiple, HTF fluid hot and cold temperature, and the receiver required thermal power to design an optimal tower and receiver. *Heat Transfer Fluid Type*: Salt (60% $NaNO_3$, 40%KNO_3) For the resulting parameters please refer to appendix A.6
Power Cycle	Refer to table 5.1.

Thermal Storage	Refer to table 5.1
System Control	In this section it is possible to specify the amount of energy that is required for the solar tracking heliostats and other parasitics. *Fraction of Rated Gross Power Consumed at All Times*: $0.0055 \frac{MW}{MW_{cap}}$
System Costs	In this section it is possible to specify both direct and indirect capital costs along with operational and maintenance costs. These figures were obtained from the Austella (2014) 'Australian Guide to SAM for Concentrating Solar Power' [20]. A sensitivity analysis is performed on these figures in section 7 of this report. *Site Improvements*: $16 \frac{\$}{m^2}$ *Heliostat Cost*: $170 \frac{\$}{m^2}$ The tower and receiver costs are based on reference plants and a scaling component is added based on the relative size of the plant that is being modelled. *EPC and Owner Cost*: 11% of direct capital cost *Total Land Cost*: $10000 \frac{\$}{acre}$ **Note: It is assumed that no adjacent land is owned by the coal-fired power station companies. If the land was owned, it would lower capital costs.** *Fixed O&M by Capacity*: $66 \frac{\$}{kW-yr}$ *Variable O&M by Generation*: $4 \frac{\$}{MWh}$ For complete system costs from SAM refer to appendix A.7.
Lifetime	Refer to table 5.1.
Financial Parameters	See section 5.2 of the report.
Time of Delivery Factors	Refer to table 5.1.
Incentives	Refer to table 5.1.
Depreciation	See section 5.2 of the report.

5.2 Financial Model

5.2.1 Financial Parameters

SAM defaults to the American tax system, so users must be careful to alter the inputs to ensure they are appropriate for projects under the Australian government. The financial parameters in this analysis were used to emulate the Australian tax system, and were suggested by the Australian Solar Thermal Energy Association [20]. The financial parameters used in both the parabolic trough and power tower modelling are detailed in table 5.4 below.

TABLE 5.4 FINANCIAL MODEL USED IN SAM

Financial Parameter	Input to SAM
IRR Target	10.29%
IRR Target Year	20 years
PPA Price Escalation Rate	1 %/year
Analysis Period	25 years
Inflation Rate	2.5%
Real Discount Rate	7.6%
Nominal Discount Rate	10.29%
Federal Income Tax Rate	30%
State Income Tax Rate	0%
Net Salvage Value	5% of installed cost
Property Tax	0% of installed cost
Loan: Debt Percent	60% of total capital cost
Loan: Tenor	15 years
Loan: Annual Interest Rate	12%

For more detailed financial parameter inputs and results refer to appendix A.8.

5.2.2 Incentives

There is an option to include government incentives or tax breaks for renewable projects, however, this has been switched off in SAM for the purpose of unbiased economic analysis.

5.2.3 Depreciation

Australia has no state income tax and as a result state depreciation is not relevant. Federal depreciation is set to a straight line over 20 years [20].

5.3 Limitations

It is important to consider the limitations of the model to ensure its results are valid. The limitations of this model include:

- *Only one year of DNI data for each location is used for modelling*. Solar radiation is constantly varying like any weather pattern. As such the annual DNI distribution in the year that was analysed will be different to future years. DNI distribution, however, is relatively predictable on a long term basis, so this minimises the effect of this limitation.
- *Uniform dispatch is used for PPA pricing however pricing events fluctuate.* It is known that electricity prices vary depending on whether electricity is in demand at a given time of day or year. Using uniform dispatch ensures constant electricity prices regardless of when it is distributed.
- *This model assumes a debt percentage of 60% of the total capital costs.* This value could vary and this would affect the cost projections.
- *This model does not take into account the cost of a control system that would be required to regulate when and how much of the extracted turbine steam is required to heat the feedwater.*

6. Results

6.1 Overview

Beyond parameters that cannot be changed such as the location and DNI resource, the most vital parameter in sizing a solar field is the solar multiple. 'The solar multiple is a measure of the solar field aperture area as a function of the power block's nameplate capacity' [21]. A solar multiple of 1 is the aperture area required of the collector to deliver enough thermal energy to the power cycle to drive it at its nameplate capacity under design conditions. In comparison, a solar farm with solar multiple 2 would have a field twice as large under the same design conditions. The design conditions refer to the 'design point irradiation' which is usually the recorded DNI at 12 noon on the equinox (approximately September 23rd in Australia) [21]. Increasing the solar multiple of a solar farm increases its capacity factor allowing it to operate at capacity for longer, however, it also increases the amount of heat energy dumped during high irradiation periods [21]. As such an optimal level must be found which minimises the cost of heating in cents/kWh.

The SAM outputs the cost of electricity produced by the designed solar field (which can be converted to cost of heating by multiplying this value by the inputted cycle conversion efficiency of 0.5). The goal of this thesis is to find the most economically viable way to integrate CSP technology with Australia's coal-fired power plants, which is achieved when the PPA cost of solar heating (cents/kWh) is minimised.

6.2 Solar Multiple Parametric Analysis

6.2.1 Parabolic Trough

A parametric analysis has been performed for parabolic trough collectors in SAM for feedwater inputs 1 and 2 and is displayed in figures 6.1 and 6.2, respectively. In this analysis, the solar multiple has been varied from 1 to 3, with the resulting PPA price of heating being recorded at each point. The lowest PPA price for heating and therefore optimal solar multiple level has been displayed of each graph.

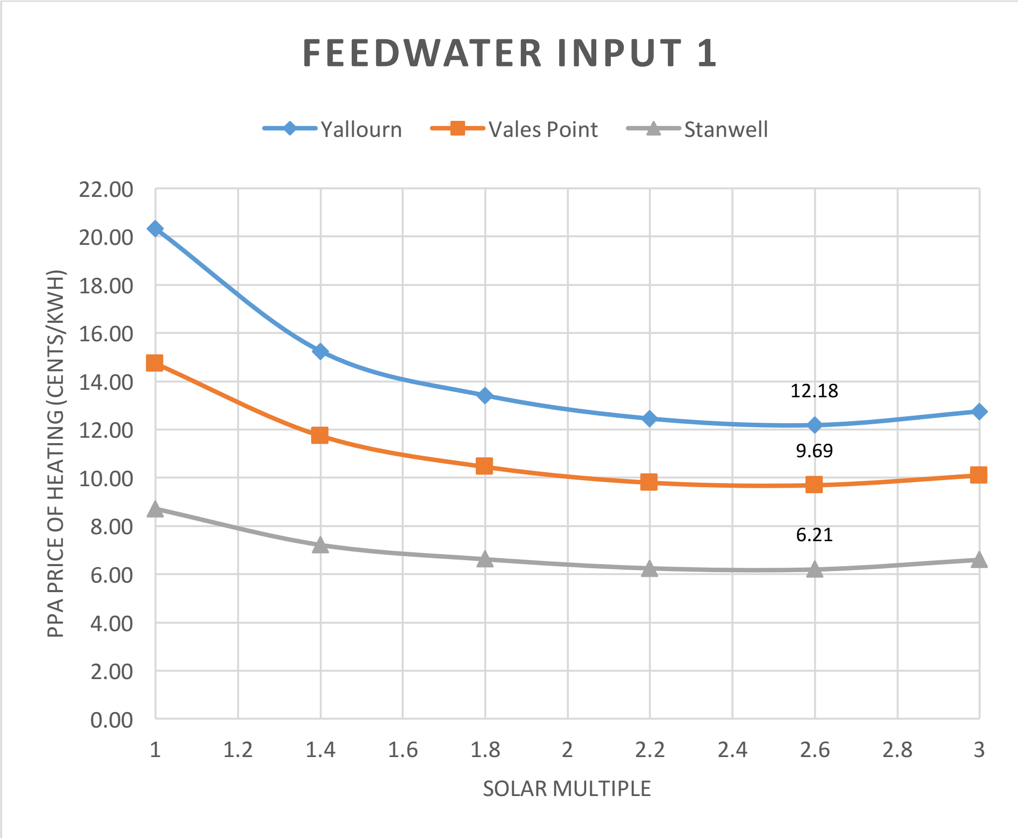

Figure 6.1: Parabolic Trough Feedwater 1 Parametric Analysis

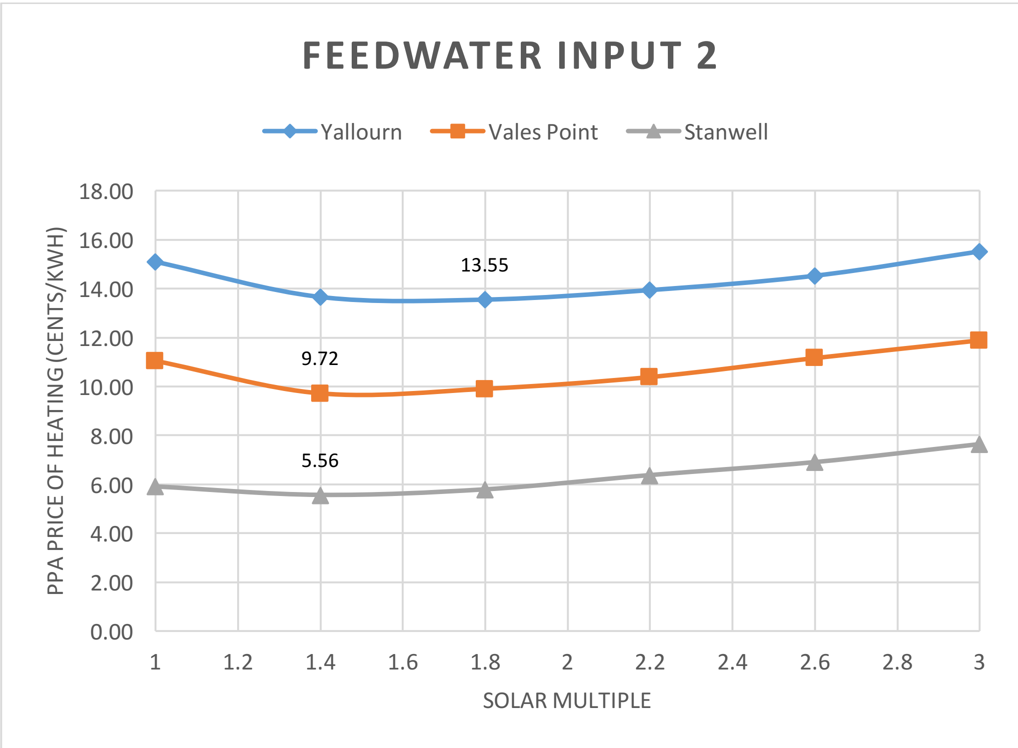

Figure 6.2: Parabolic Trough Feedwater 2 Parametric Analysis

6.2.2 Power Tower

A parametric analysis has been performed for power tower collectors in SAM for feedwater inputs 1 and 2 and is displayed in figures 6.3 and 6.4, respectively. In this analysis, the solar multiple has been varied from 1 to 3, with the resulting PPA price of heating being recorded at each point. The lowest PPA price for heating and therefore optimal solar multiple level has been displayed of each graph.

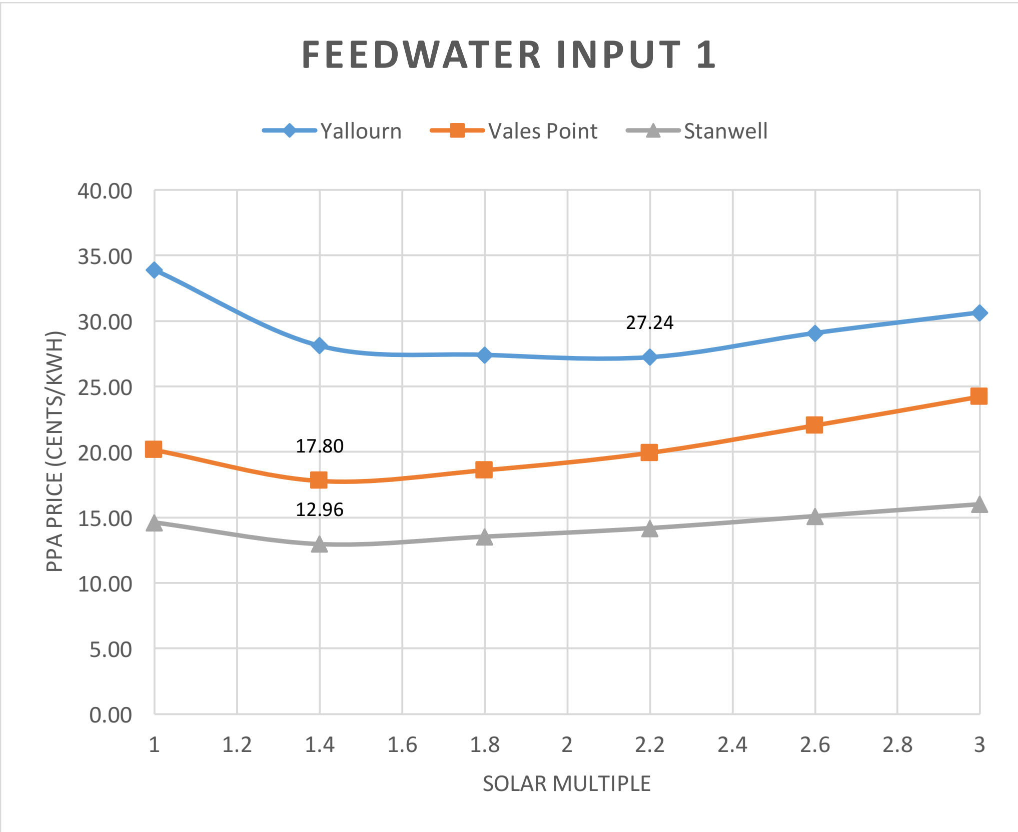

Figure 6.3: Power Tower Feedwater 1 Parametric Analysis

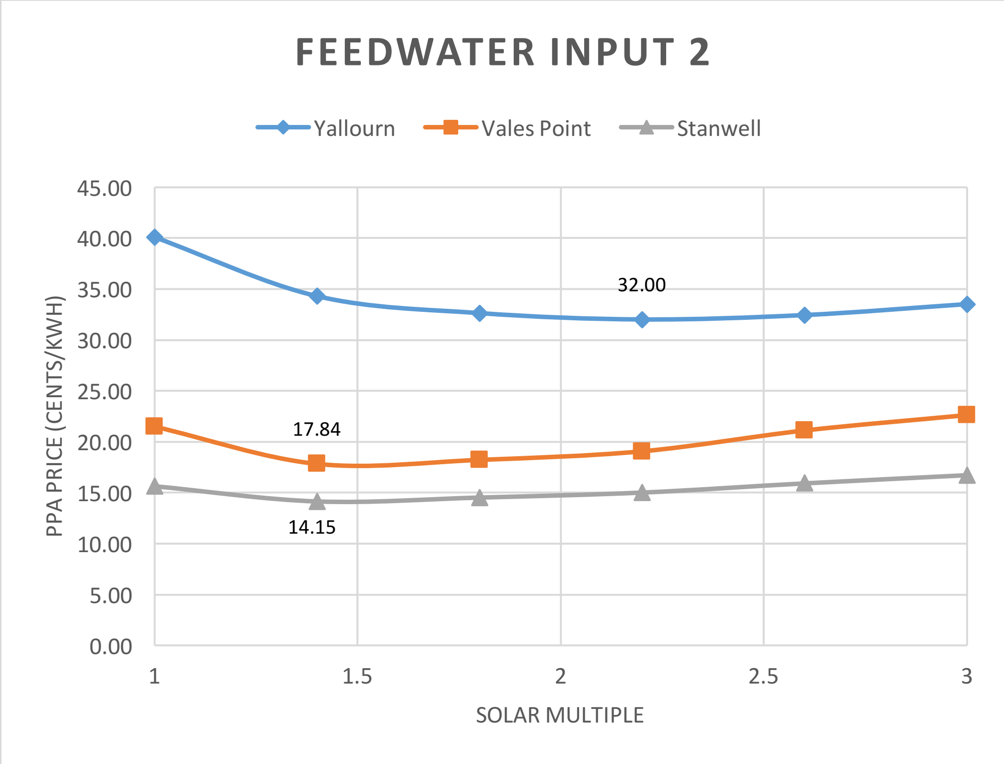

Figure 6.4: Power Tower Feedwater 2 Parametric Analysis

6.3 Final Results

The results for all systems at their optimal solar multiple is displayed below in table 6.1. The mean DNI of each power plant's location resource has been provided in column one to compare against the resulting PPA price of heating for each solar field.

TABLE 6.1 FINAL SAM OUTPUTS

Power Plant	Feedwater Input	Collector Type	Solar Multiple	Annual Heating Output (GWh)	Capacity Factor (%)	PPA Price of Heating (cents/kWh)
Stanwell Mean DNI = 268.2 (W/m^2)	Feedwater 1	Parabolic Trough	2.6	104.6	30.2	**6.21**
		Power Tower	1.4	81.7	23.6	**12.96**
		Difference (Trough-Tower)	-	22.9	6.6	**-6.75**
	Feedwater 2	Parabolic Trough	1.4	59.5	22.3	**5.56**
		Power Tower	1.4	63	23.5	**14.15**
		Difference (Trough-Tower)	-	-3.5	-1.2	**-8.59**

Power Plant	Feedwater Input	Collector Type	Solar Multiple	Annual Heating Output (GWh)	Capacity Factor (%)	PPA Price of Heating (cents/kWh)
Vales Point Mean DNI = 165.8 (W/m^2)	Feedwater 1	Parabolic Trough	2.6	129.5	19.2	**9.69**
		Power Tower	1.4	105.2	15.6	**17.80**
		Difference (Trough-Tower)	-	24.3	3.6	**-8.11**
	Feedwater 2	Parabolic Trough	1.4	59.3	12.3	**9.72**
		Power Tower	1.4	74.9	15.6	**18.68**
		Difference (Trough-Tower)	-	-15.6	-3.3	**-8.96**
Yallourn Mean DNI = 134 (W/m^2)	Feedwater 1	Parabolic Trough	2.6	50.5	15.4	**12.18**
		Power Tower	2.2	43.8	13.3	**28.53**
		Difference (Trough-Tower)	-	6.7	2.1	**-16.35**
	Feedwater 2	Parabolic Trough	1.8	25.7	10.6	**13.55**
		Power Tower	2.2	30.7	12.7	**32.00**
		Difference (Trough-Tower)	-	-5	-2.1	**-18.45**

It can be seen from table 6.1 that there is a correlation between the 'mean DNI' at a given resource and the resulting PPA price of heating. Plants with higher 'mean DNI' result in a lower PPA price of heating as the solar resource is greater. Furthermore, for all locations and feedwater solar inputs, power tower models resulted in a PPA price of heating that was at least two times larger than the parabolic trough alternative model. This is largely due to the fact that the capital cost for power tower systems is significantly more expensive than parabolic trough systems. Also, power tower systems generally become cost effective at the utility-scale of size greater than 50MW which is substantially larger than the plants being modelled [22]. In addition to this, both the power tower model and parabolic trough model resulted similar annual heating output and capacity factor values. These factors indicate that the most appropriate solar collector type for this application in Australia is the parabolic trough collector.

7. Economic Analysis

7.1 Parabolic Trough Versus Power Tower

It is clear from section 6.3 that in every simulation the PTC system is a more economically competitive solution when compared to the power tower model. This is largely due to the fact that the capital cost of power tower systems is substantially higher when compared to PTCs, however, this increase in cost results in little, if any, gains on heat energy produced and capacity factor (see section 6.3). A comparison of net capital costs of each power tower system when compared to the parabolic trough alternative for feedwater inputs 1 and 2 is provided in figure 7.1 and 7.2, respectively.

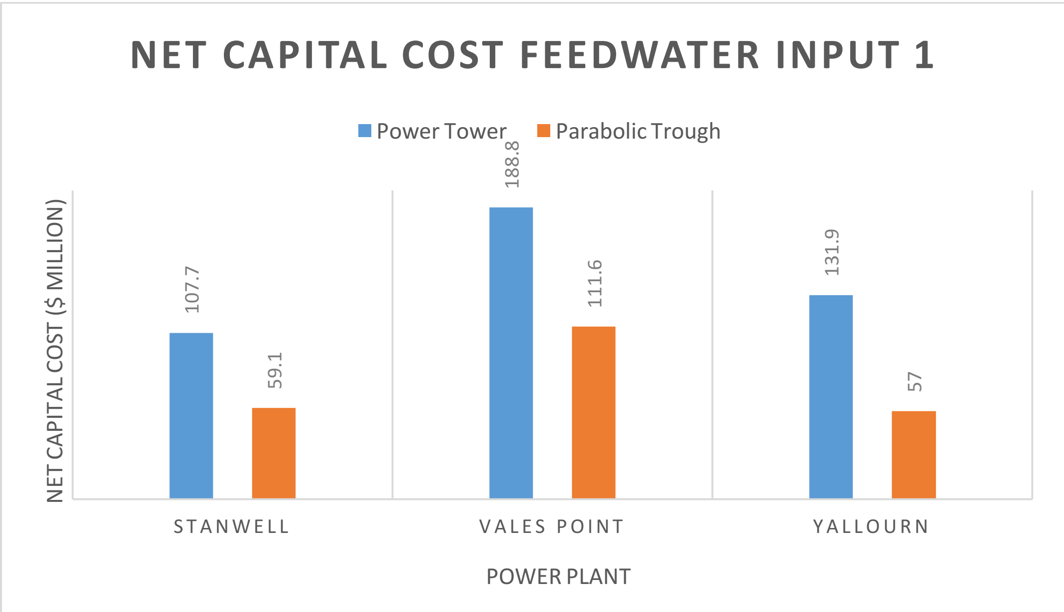

Figure 7.1 Net Capital Cost Feedwater Input 1 Comparison

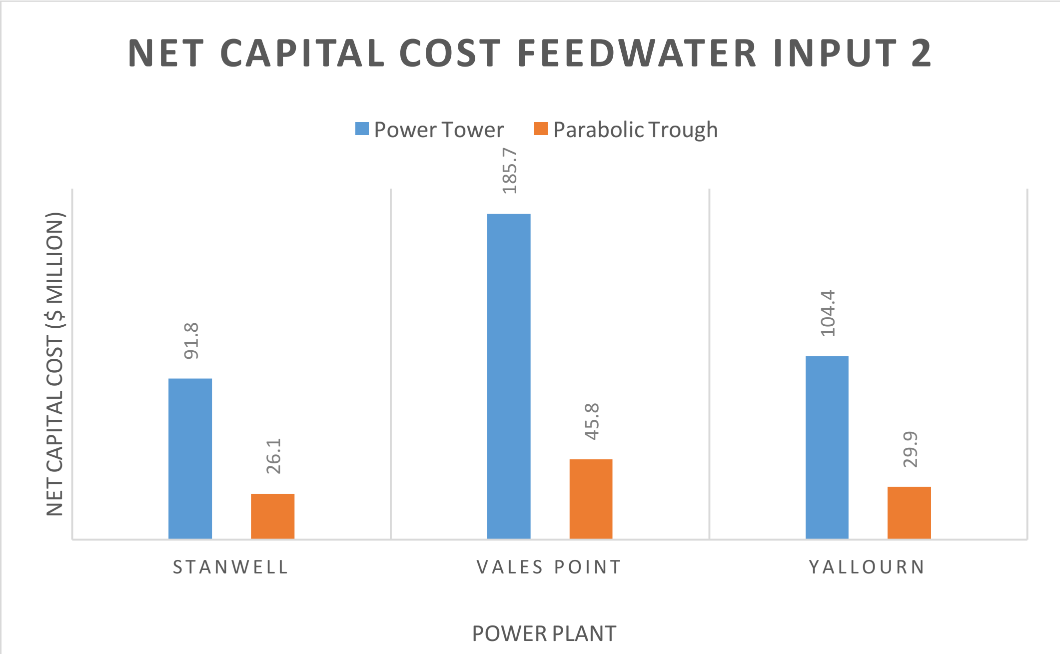

Figure 7.2 Net Capital Cost Feedwater Input 2 Comparison

7.2 Sensitivity Analysis

As a result of their economic dominance, the PTC system is chosen to be the collector type most useful for integration into Australia's coal-fired power plants. The two most influential parameters in the capital cost calculation of a PTC system are the solar field cost $(\frac{\$}{m^2})$ and the heat transfer system cost $(\frac{\$}{m^2})$, together making up approximately 70% of the total capital cost. As such, a sensitivity analysis was performed on these parameters to indicate the effect that changing them would have on the PPA price of heating. Table 7.1 details the value for the solar field cost and heat transfer fluid system cost that was used in the modelling, along with an upper and lower bound for each. The resulting parametric analysis for Stanwell, Vales Point, and Yallourn power stations is displayed in figures 7.3, 7.4, and 7.5, respectively.

TABLE 7.1 ECONOMIC PARAMETRIC ANALYSIS INPUT PARAMETERS

Parameter	Lower Bound	Actual Value	Upper Bound
Solar Field Cost $(\frac{\$}{m^2})$	120	170	220
Heat Transfer System cost $(\frac{\$}{m^2})$.	50	70	90

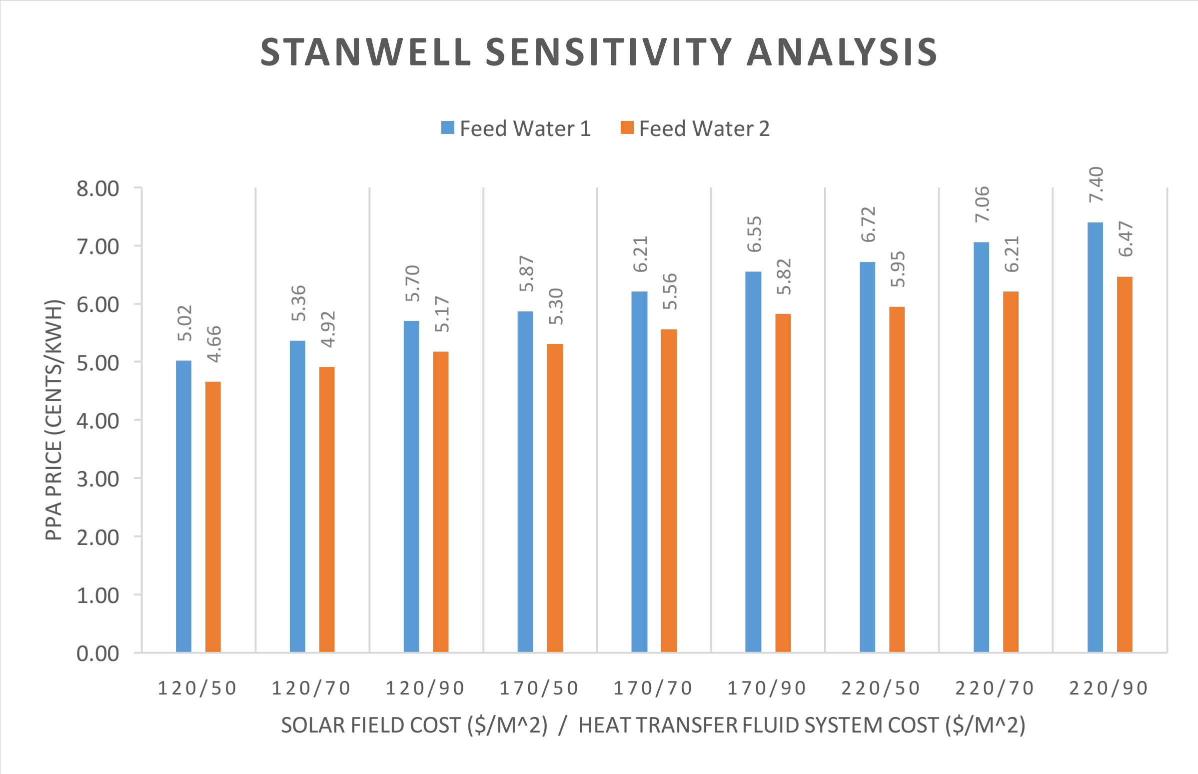

Figure 7.3 Stanwell Sensitivity Analysis

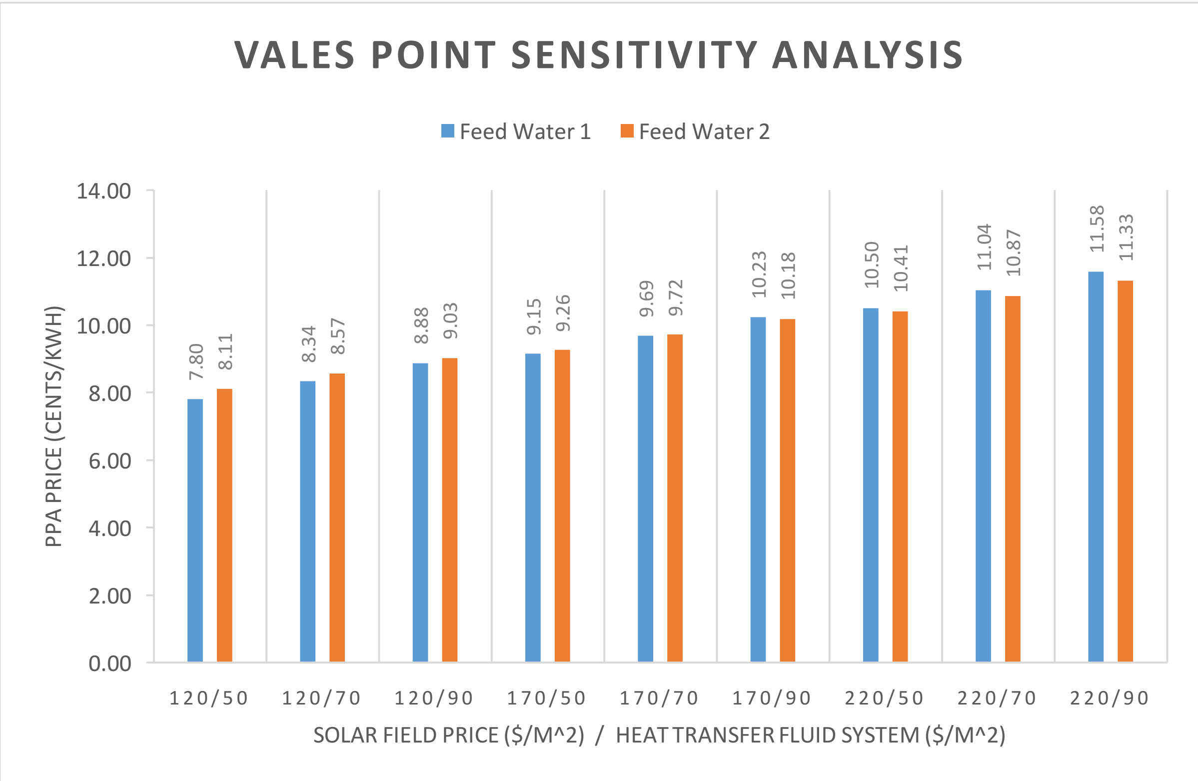

Figure 7.4 Vales Point Sensitivity Analysis

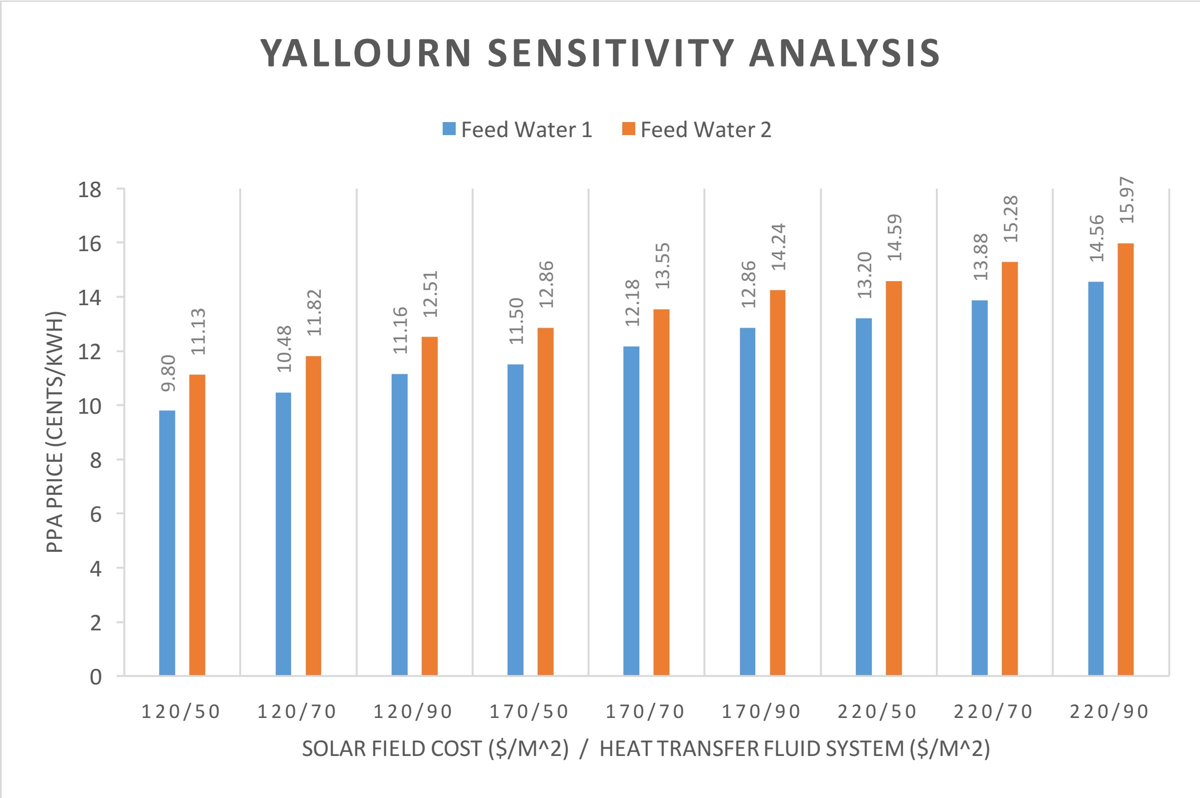

Figure 7.5 Yallourn Sensitivity Analysis

Evidently, increasing the price of either the solar field cost or heat transfer system cost increases the PPA price of heating for the given solar field. From the cheapest (solar field $120\frac{\$}{m^2}$ / heat transfer system $50\frac{\$}{m^2}$) to most expensive (solar field $220\frac{\$}{m^2}$ / heat transfer system $90\ \frac{\$}{m^2}$) combination there is a PPA heating price jump of 50% or more in every case. Therefore, as the price of PTC systems and their corresponding heat transfer fluid system continues to fall into the future, the PPA cost of heating will become more economically competitive.

7.3 Energy Production Costs

To this point in the report, only the cost of heating has been analysed and optimised. The next stage of the analysis is to determine the cost of electricity production from the solar field. SAM outputs provide an annual levelised cost of heating for each parabolic trough solar field and these values are detailed below in table 7.2.

TABLE 7.2 ANNUAL LEVELISED HEATING COSTS FOR PTCS

Power Plant	Feedwater Input	Annual Levelised Heating Cost ($ million)
Stanwell	1	6.5
	2	3.311
Vales Point	1	12.56
	2	5.763
Yallourn	1	6.148
	2	3.476

Next it is necessary to calculate the electricity that the steam left un-extracted would produce when the solar farm is providing the heating for the feedwater. The annual electricity produced from the un-extracted steam can be calculated using the following equation:

$$Electricity\ from\ steam_{annual} = \dot{m} \times (h_i - h_o) \times 365 days \times 24 hours \times Gen_{eff} \times CAPF \quad (5)$$

Where;

$\dot{m}$ = mass flow rate of steam $\left({}^{kg}/_{s}\right)$,

h_i = Input enthalpy of the steam $\left({}^{kJ}/_{kg}\right)$,

h_o = Output enthalpy of the steam after passing through the turbine $\left({}^{kJ}/_{kg}\right)$,

Gen_{eff} = Generator efficiency of the coal-fired power plant,

$CAPF$ = Capacity factor of the PTC plant,

$Electricity\ from\ steam_{annual}$ = Electricity produced by un-extracted steam (kWh).

Now, to determine the cost of electricity (in cents/kWh) produced from the solar farm, the following equation can be used:

$$Solar_{cost} = \frac{Annual\ levelised\ heating\ cost\ from\ solar}{Electricity\ from\ steam_{annual}} \quad (6)$$

Table 7.3 details all parameters of the last two equations which are used to calculated the cost of energy produced by the solar field.

TABLE 7.3 SOLAR ELECTRICITY COST CALCULATIONS

Power Plant	**Stanwell**		**Vales Point**		**Yallourn**	
Feedwater Input	1	2	1	2	1	2
Extraction Steam Mass Flow Rate (kg/s)	23.235	16.254	45.39	29.21	21.951	14.595
Steam Enthalpy Input (kJ/kg)	3532.5	3368.1	3532	3375	3533	3350
Steam Enthalpy Output (kJ/kg)	2372.3		2384		2398	
Generator Efficiency (%)	98.8		99		98.8	
Solar Plant Capacity Factor (%)	30.2	22.3	19.2	12.3	15.4	10.6
Annual Electricity from Steam (GWh)	52.30	31.24	86.59	30.82	33.21	12.75
Annual Levelised Cost of Solar Heating ($ million)	6.5	3.311	12.56	5.763	6.148	3.476
Solar Electricity Cost (cents /kWh)	**9.22**	**10.6**	**14.5**	**18.7**	**18.5**	**27.3**

It is important to compare the cost of producing electricity from each solar integrated plant to both the cost of producing electricity from coal and the cost of producing electricity from stand-alone PTC systems.

The cost of producing electricity from coal varies depending on the fluctuating price of coal, however, an average value of 4 $\frac{cents}{kWh}$ is attained from the Australian Bureau of Resources and Energy Economic (BREE) [23]. Clearly, none of the integrated solar power plants attains this value, with the closest integrated plant 'feedwater 1 integration in Stanwell' attaining a price that is just over twice as expensive. This makes the solar integration system economically less appealing when compared to leaving the coal plant to operate as normal. It is important to note that if the Australia government were to introduce a carbon tax or emissions trading scheme, then the price of electricity production from coal would inevitably increase. In this case, this solar integration cost would become more competitive as a result of its low emissions.

In contrast to coal electricity prices, the levelised cost of energy from stand-alone PTC systems in Australia (with a power cycle attached) was approximately $30 \frac{cents}{kWh}$ in 2012 [24]. All simulated PTC solar-coal hybrid systems attain an electricity cost less than this, with the 'feedwater 1 integration in Stanwell' achieving under a third of this cost. It is therefore clear that PTC solar-coal integrated systems are more economically competitive than stand-alone PTC systems. This is due to the fact that in the integrated system the solar to electric efficiency is not limited by the temperature of the solar heat and also there is no need to build an additional power cycle.

8. Environmental Analysis

8.1 Overview

Traditional coal-fired power plants have a high intensity emissions rating, and as a result they are the nation's top source of CO_2 emissions [25]. In comparison, CSP technologies are clean energy sources, with no emissions. As a result of this, the integration of CSP to Australia's coal-fired power plants would result in a significant reduction in emissions. This would contribute to Australia's current goal of a 28% reduction in emissions by 2030 [25].

8.2 CO2 Emissions

An annual report by the 'National Greenhouse and Energy Reporting' (NGER) government clean energy regulator details figures on the amount of CO_2 emissions each coal-fired power station in Australia produced in 2014 [26]. The total amount of avoided CO_2 emissions from the proposed integrated plant can be calculated by multiplying this intensity factor by the amount of annual electricity saved because of the heating provided by each PTC field.

TABLE 8.1 CO_2 EMISSIONS AVOIDED BY SOLAR INTEGRATION [26]

Power Station	Feedwater Input	Annual Solar Electricity Produced (MWh)	Power Station Coal Type	Power Station Emission Intensity $(tonnes CO_2/MWh)$	CO_2 avoided (tonnes)	Percent of total Annual Power Plant Emissions (%)
Stanwell	1	52,300	Black Coal	0.86	44,978	0.87
	2	31,240			26,866	0.52
	Total	83,540			71,844	1.39
Vales Point	1	86,590	Black Coal	0.87	75,333	1.44
	2	30,820			26,814	0.51
	Total	117,410			102,147	1.95
Yallourn	1	33,120	Brown Coal	1.27	42,062	0.55
	2	12,750			16,193	0.21
	Total	45,870			58,255	0.76

Clearly, Yallourn power station, which runs on brown coal has a much higher emissions intensity factor than both Stanwell and Vales Point power stations that both run on black coal. Solar integration in brown coal power plants therefore has a more beneficial environmental impact when compared to integration in black coal stations.

The total amount of emissions avoided are only a small fraction of each power plant's annual emissions, however, they are all still significant values.

9. Conclusions

In this paper, three of Australia's coal fired power plants (Stanwell, Vales Point, and Yallourn) were used to determine the potential for CSP integration with Australia's coal-fired power plants. Throughout this investigation, various important conclusions were reached:

- Parabolic trough collector systems are the most useful and cost effective solar collector type for this application.
- Feedwater heating integration is the most cost effective solar input into Australia's coal fired power plants.
- Each power plant's DNI resource is the most crucial factor in determining the feasibility a proposed solar integration project.
- Electricity produced by solar integration is currently more expensive than electricity produced by coal alone, however, it is far more competitive than stand-alone CSP plants.
- Solar-coal integration plants could be used as an effective means of emissions reduction.

Figure 9.1 details the relationship between the mean DNI at each analysed coal-fired power station and the resulting solar electricity PPA price. A negative-power trend line has been fitted to the data. This relationship will be used to extend this investigation to Australia's coal-fired power plants that were not analysed.

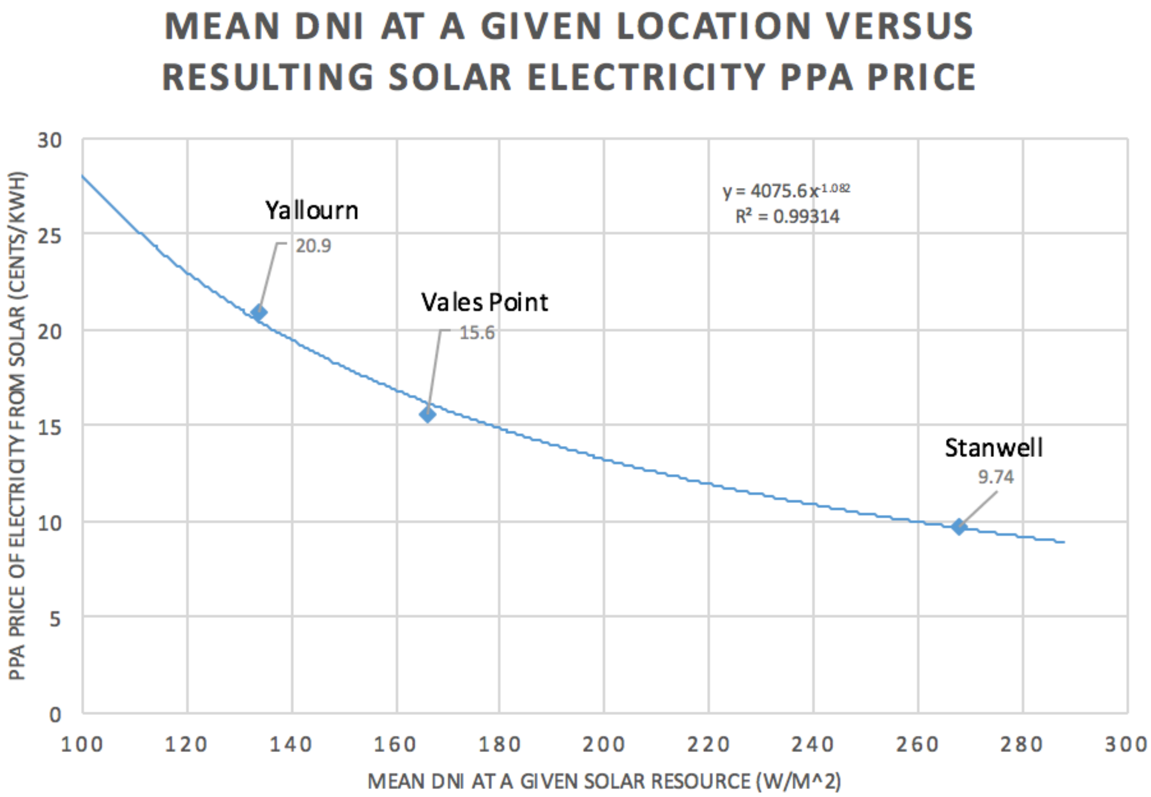

Figure 9.1 Mean DNI at a Given Location Versus Resulting Solar Electricity PPA Price

Table 9.1 uses the trend line equation from figure 9.1 to calculate the expected PPA price of solar electricity if integration were to occur at each coal-fired power station in Australia. Each coal-fired power station in Australia has also been given a 'solar integration potential' rating depending on the estimated PPA price of its resulting solar electricity: less than 10cents/kWh = Excellent, between 10 and 15 cents/kWh = good, between 15 and 20 cents/kWh = fair, and over 20 cents/kWh = poor. These estimates are rough, and are based solely on the power plants mean DNI data at the closest location with solar data available. It would be beneficial for this table to be updated with more accurate solar resource data if these become available in the future. Furthermore, as seen in this report, numerous other factors affect the PPA price of electricity modelling such as; plant capacity, power plant configuration and efficiencies, and feedwater extraction steam properties. Therefore, the solar integration potential should only be used as an indication as to whether further, more complete analysis should be performed on each power plant using the methods carried out in this report for Stanwell, Vales Point, and Yallourn power stations.

TABLE 9.1 SOLAR INTEGRATION POTENTIAL OF AUSTRALIA'S COAL-FIRED POWER PLANTS

State	Power Station and Capacity (MW)	Closest Solar Resource and Distance Away (km)	Mean DNI at Closest Resource $\left({W}/{m^2}\right)$	Estimated PPA Price of Solar Electricity (cents/kWh)	Solar Integration Potential
QLD	Collinsville (190)	Longreach, QLD (600)	294	8.7	Excellent
	Tarong North (443)	Chinchilla, QLD (160)	268	9.74	Excellent
	Callide A & B (730)	Chinchilla, QLD (350)	268	9.74	Excellent
	Kogan Creek (750)	Chinchilla, QLD (25)	268	9.74	Excellent
	Millmerran (852)	Chinchilla, QLD (170)	268	9.74	Excellent
	Callide C (900)	Chinchilla, QLD (350)	268	9.74	Excellent
	Tarong (1400)	Chinchilla, QLD (150)	268	9.74	Excellent
	Stanwell (1445)	Chinchilla, QLD (460)	268	9.74	Excellent
	Gladstone (1680)	Chinchilla, QLD (480)	268	9.74	Excellent
NSW	Vales Point (1320)	Sydney, NSW (120)	166	15.6	Fair
	Mt Piper (1400)	Sydney, NSW (160)	166	15.6	Fair
	Liddell (2000)	Sydney, NSW (240)	166	15.6	Fair
	Bayswater (2640)	Sydney, NSW (240)	166	15.6	Fair
	Eraring (2880)	Sydney, NSW 140)	166	15.6	Fair
VIC	Hazelwood (1600)	Melbourne, VIC (140)	134	20.9	Poor
	Loy Yang A (2200)	Melbourne, VIC (160)	134	20.9	Poor

State	Power Station and Capacity (MW)	Closest Solar Resource and Distance Away (km)	Mean DNI at Closest Resource $\left(W/_{m^2}\right)$	Estimated PPA Price of Solar Electricity (cents/kWh)	Solar Integration Potential
	Loy Yang B (1050)	Melbourne, VIC (160)	134	20.9	Poor
	Yallourn (1480)	Melbourne, VIC (140)	134	20.9	Poor
SA	Northern (520)	Port Augusta, SA (9)	260	9.94	Excellent
	Playford B (240)	Port Augusta, SA (12)	260	9.94	Excellent
WA	Worsley (107)	Perth, WA (190)	222	11.8	Good
	Collie (300)	Perth, WA (210)	222	11.8	Good
	Bluewaters (416)	Perth, WA (200)	222	11.8	Good
	Kwinana (640)	Perth, WA (35)	222	11.8	Good
	Muja (854)	Perth, WA (220)	222	11.8	Good

References

[1] V. Davli, “Nature Climate Change,” Nature Climate Change, 2015. [Online]. Available: http://www.nature.com/nclimate/journal/v5/n11/full/nclimate2717.html. [Accessed 4 April 2016].

[2] ARENA, “Solar Energy,” 2011. [Online]. Available: http://arena.gov.au/files/2013/08/Chapter-10-Solar-Energy.pdf. [Accessed 10 May 2016].

[3] NREL, “Solar-Fossil Integration Plants,” 2015. [Online]. Available: http://www.nrel.gov/csp/solarpaces/project_detail.cfm/projectID=44. [Accessed 2 October 2016].

[4] U. D. o. Energy, “Sunshot Vision Study,” 2012. [Online]. Available: http://energy.gov/sites/prod/files/SunShot%20Vision%20Study.pdf. [Accessed 14 April 2016].

[5] IRENA, “Concentrating Solar Power,” 2012. [Online]. Available: http://www.irena.org/documentdownloads/publications/re_ technologies_cost_analysis-csp.pdf. [Accessed 16 April 2016].

[6] J. Hinkley, “Concentrating solar power - drivers and opportunities for cost-competitve electricity,” 2011. [Online]. Available: http://www.garnautreview .org.au/update-2011/commissioned-work/concentrating-solar-power-drivers-opportunities-cost-competitive-electricity.pdf. [Accessed 14 April 2016].

[7] L. Hubb, “Solar Thermal for Electricity,” 2016. [Online]. Available: http://greenterrafirma.com/solar-thermal-for-electricity.html. [Accessed 2 April 2016].

[8] L. Riyad, “Parabolic Dish System,” 2012. [Online]. Available: https://shaikmohasin.wordpress.com/page/10/?archives-list=1. [Accessed 14 April 2016].

[9] U. D. o. Energy, “Linear Concentrator System Basics for Concentrating Solar Power,” 2013. [Online]. Available: http://energy.gov/eere/energybasics/articles/linear -concentrator-system-basics-concentrating-solar-power. [Accessed 10 April 2016].

[10] S. Benmarraze, “Linear Fresnel Reflectors Concenctrated Solar Power: Cost Reduction and Performance Improvement Trends,” 2015. [Online]. Available: http://costing.irena.org/media/9984/20150319_SEM_IRENA%20LFR%20Presentation _print.pdf. [Accessed 22 April 2016].

[11] ENGIE, “Coal-Fired Power Station,” 2016. [Online]. Available: http://www.gdfsuezau.com/education/Coal-fired-Power-Station. [Accessed 4 May 2016].

[12] A. Neville, “Martin Next Generation Solar Energy Centre,” 2011. [Online]. Available: http://www.powermag.com/top-plantmartin-next-generation-solar-energy-center-indiantown-martin-county-florida/?pagenum=3. [Accessed 13 October 2016].

[13] H. Hongjuan, “Solar-Coal Hybrid Thermal Power Generation - an Efficient Way to Use Solar Energy in China,” *International Journal of Energy Engineering,* vol. VI, pp. 50-55, 2011.

[14] Newport, "Introduction to Solar Radiation," 2016. [Online]. Available: https://www.newport.com/introduction-to-solar-radiation. [Accessed 24 May 2016].

[15] M. Gunther, "Advanced CSP Teaching Materials: Solar Radiation," 2014. [Online]. Available: http://www.energy-science.org/bibliotheque/cours/1361469594 Chapter%2002%20radiation.pdf. [Accessed 15 May 2016].

[16] BOM, "Solar Radiation Definitions," 2012. [Online]. Available: http://www.bom.gov.au/climate/austmaps/solar-radiation-glossary.shtml. [Accessed 2 May 2016].

[17] D. Brooks, "Notes From a Temperate Climate," 2008. [Online]. Available: http://www.instesre.org/TemperateClimate/TemperateClimate.htm. [Accessed 24 May 2016].

[18] K. &. Zonnen, "Pyrheliometer," 2016. [Online]. Available: http://www.kippzonen.com/Product/18/CHP1-Pyrheliometer #.V0-RyFf62mA. [Accessed 22 May 2016].

[19] R. Bingh, "Plants in Australia," 2016. [Online]. Available: http://www.industcards.com/ppworld.htm. [Accessed 29 March 2016].

[20] NREL, "National Solar Radiation Database," 2016. [Online]. Available: https://nsrdb.nrel.gov/archives. [Accessed 28 may 2016].

[21] NREL, "Engineering and Techno-Economic Assessment," 2016. [Online]. Available: http://www.nrel.gov/csp/engineering-techno-economic-analysis.html. [Accessed 5th September 2016].

[22] Austella, "Australia Companion Guide to SAM for Concentrating Solar Power," IT Power, 2014. [Online]. Available: http://www.austela.com.au/docs/projects /sam/SAM_for_Aus_Companion_Guide_20140306.pdf. [Accessed 1st September 2016].

[23] F. Trieb, "Global Potential of Concentrating Solar Power," 2009. [Online]. Available: http://www.solarthermalworld.org/sites/gstec/files/global%20 potential%20csp.pdf. [Accessed 14 May 2016].

[24] D. Kearney, "Utility-Scale Power Tower Solar Systems," NREL, 2013. [Online]. Available: http://www.nrel.gov/docs/fy13osti/57272.pdf. [Accessed 20 June 2016].

[25] BREE, "Australian Energy Technology Assessment," Australia Government, 2012. [Online]. Available: http://www.industry.gov.au/Office-of-the-Chief-Economist/Publications/Documents/aeta/australian_energy_ technology_assessment.pdf. [Accessed 10 October 2016].

[26] IRENA, "Renewable Energy Technologies: Cost Analysis Series," 2012. [Online]. Available: http://www.irena.org/documentdownloads/publications/re_ technologies_cost_analysis-csp.pdf. [Accessed 16 September 2016].

[27] S. Vorath, "Australia's Top 20 Greenhouse Gas Emitters," 2014. [Online]. Available: http://reneweconomy.com.au/graph-of-the-day-australias-top-20-greenhouse-gas-emitters-98644/. [Accessed 27 September 2016].

[28] NGER, "Corporate Emissions and Energy Data," Australian Government, 2015. [Online]. Available: http://www.cleanenergyregulator.gov.au/NGER/National%20greenhouse %20and%20energy%20reporting%20data/Corporate%20emissions%20and%20energy %20data/corporate-emissions-and-energy-data-2014-15. [Accessed 1 October 2016].

Appendices

Appendix A – SAM Input Parameters

A.1 Parabolic Trough Solar Field Inputs

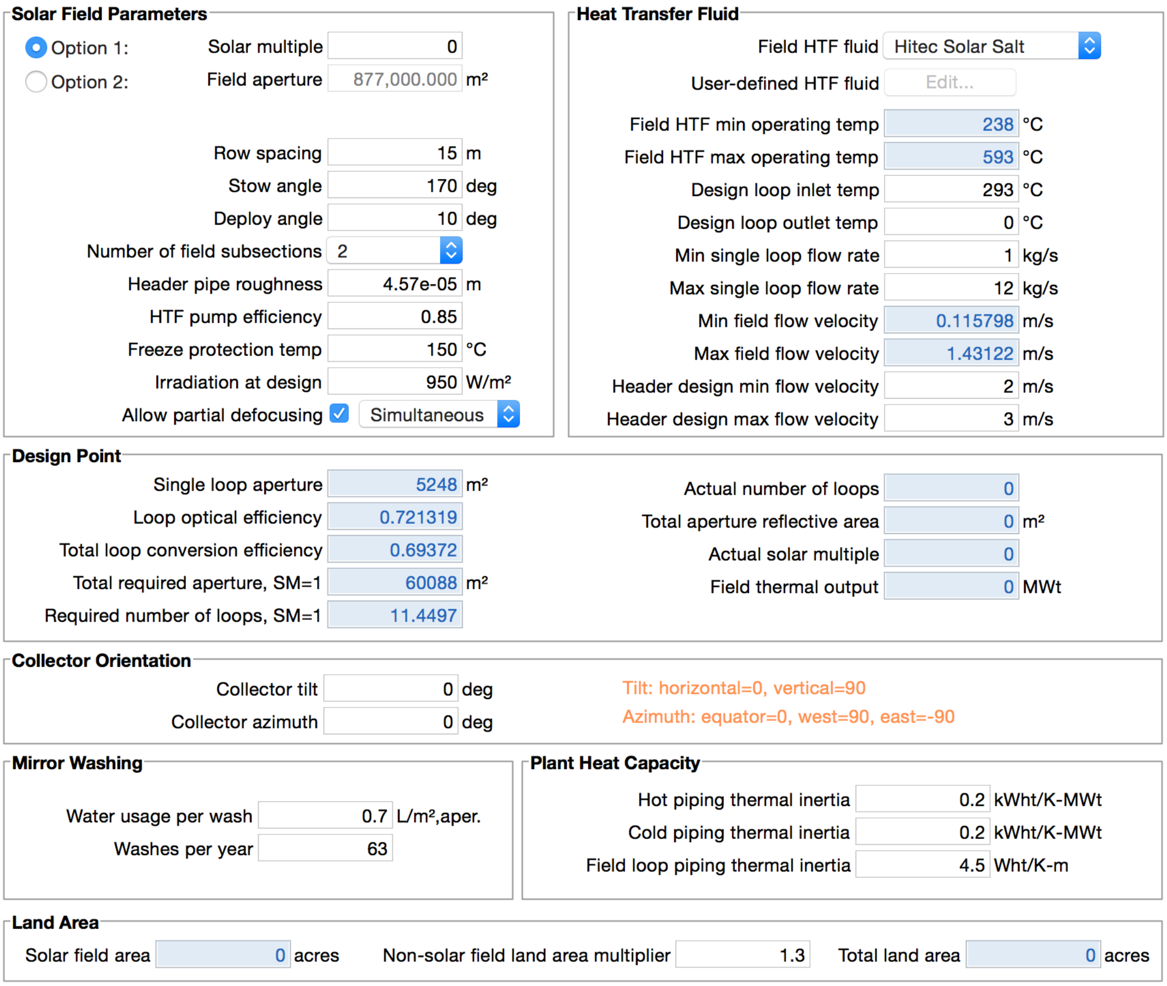

A.2 Parabolic Trough Collector Parameters

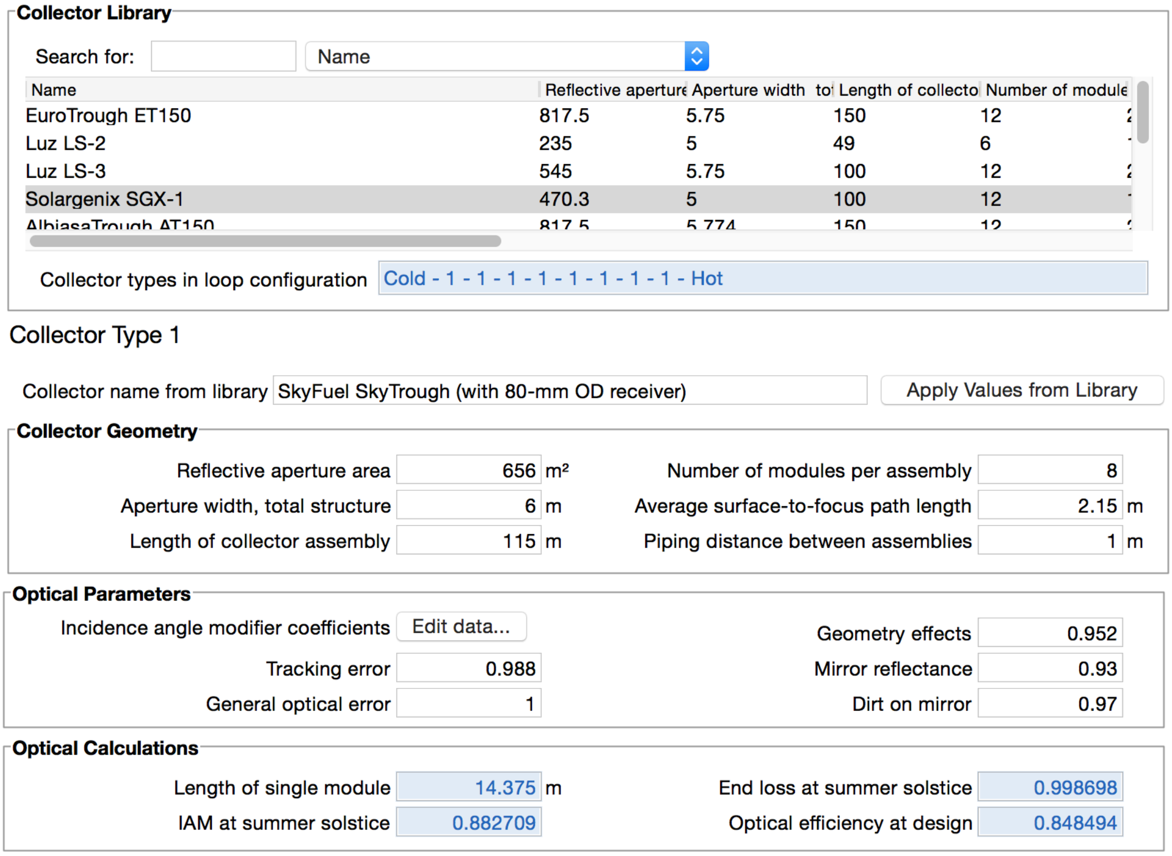

A.3 Parabolic Trough Receiver Parameters

Receiver Library

Search for: Name

Name	Absorber tube inn	Absorber tube out	Glass envelope in	Glass envelope ou	
Schott PTR70 2008	0.066	0.07	0.115	0.12	0
Solel UVAC 3	0.066	0.07	0.115	0.121	0
Siemens UVAC 2010	0.066	0.07	0.109	0.115	0
Schott PTR80	0.076	0.08	0.115	0.12	0

Receiver types in loop configuration: Cold - 1 - 1 - 1 - 1 - 1 - 1 - 1 - 1 - Hot

Receiver Type 1

Receiver name from library: Schott PTR80 — Apply Values from Library

Receiver Geometry

Absorber tube inner diameter	0.076 m	Absorber flow plug diameter	0 m
Absorber tube outer diameter	0.08 m	Internal surface roughness	4.5e-05
Glass envelope inner diameter	0.115 m	Absorber flow pattern	Tube flow
Glass envelope outer diameter	0.12 m	Absorber material type	304L

Parameters and Variations

	Variation 1	**Variation 2**	**Variation 3**	**Variation 4***
Variant weighting fraction*	0.985	0.01	0.005	0
Absorber Parameters:				
Absorber absorptance	0.963	0.963	0.8	0
Absorber emittance	Table...	0.65	0.65	0
Envelope Parameters:				
Envelope absorptance	0.02	0.02	0	0
Envelope emittance	0.86	0.86	1	0
Envelope transmittance	0.964	0.964	1	0
Broken Glass	☐	☐	☑	☐
Gas Parameters:				
Annulus gas type	Hydrogen	Air	Air	Hydrogen
Annulus pressure (torr)	0.0001	750	750	0

A.4 Parabolic Trough Power Cycle Parameters

Rankine Cycle and Hybrid Cooling

Plant Capacity

Design gross output	19.8	MWe
Estimated gross to net conversion factor	1	
Estimated net output at design (nameplate)	20	MWe

Parasitic losses typically reduce net output to approximately 90 % of design gross power

Availability and Curtailment

Curtailment and availability losses reduce the system output to represent system outages or other events.

Edit losses...

Constant loss: 4.0 %
Hourly losses: None
Custom periods: None

Power Block Design Point

Rated cycle conversion efficiency	0.5	
Design inlet temperature	0	°C
Design outlet temperature	293	°C
Fossil backup boiler LHV efficiency	1	
Aux heater outlet set temp	391	°C
Fossil dispatch mode	Minimum backup level	

Plant Control

Low resource standby period	2	hrs
Fraction of thermal power needed for standby	0.2	
Power block startup time	0.5	hr
Fraction of thermal power needed for startup	0.2	
Minimum required startup temp	300	'C
Max turbine over design operation	1.05	
Min turbine operation	0.25	

A.5 Power Tower Heliostat Field Parameters

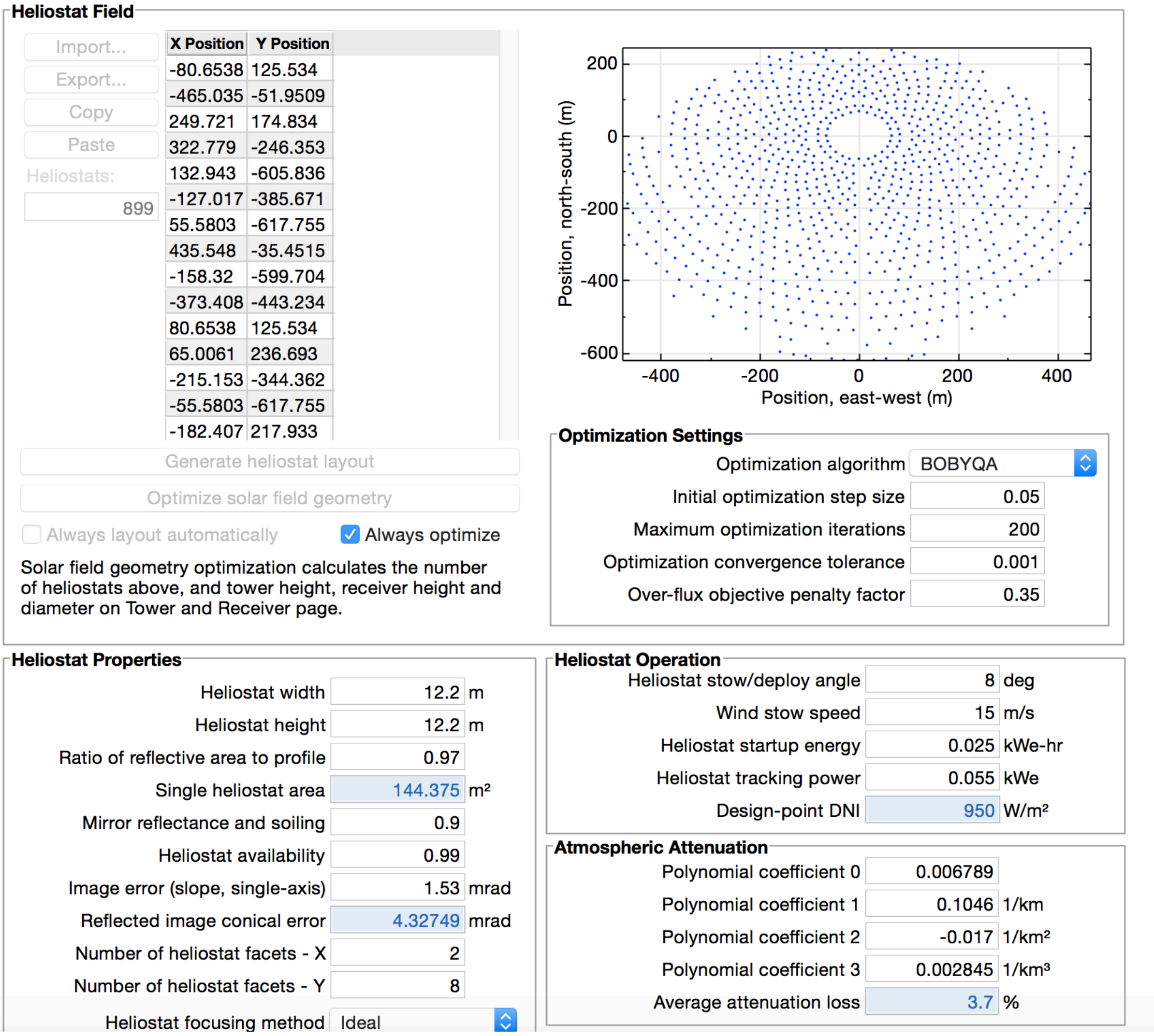

Heliostat Field

Import... Export... Copy Paste

Heliostats: 899

X Position	Y Position
-80.6538	125.534
-465.035	-51.9509
249.721	174.834
322.779	-246.353
132.943	-605.836
-127.017	-385.671
55.5803	-617.755
435.548	-35.4515
-158.32	-599.704
-373.408	-443.234
80.6538	125.534
65.0061	236.693
-215.153	-344.362
-55.5803	-617.755
-182.407	217.933

Generate heliostat layout

Optimize solar field geometry

☐ Always layout automatically ☑ Always optimize

Solar field geometry optimization calculates the number of heliostats above, and tower height, receiver height and diameter on Tower and Receiver page.

Optimization Settings

Optimization algorithm	BOBYQA
Initial optimization step size	0.05
Maximum optimization iterations	200
Optimization convergence tolerance	0.001
Over-flux objective penalty factor	0.35

Heliostat Properties

Heliostat width	12.2	m
Heliostat height	12.2	m
Ratio of reflective area to profile	0.97	
Single heliostat area	144.375	m²
Mirror reflectance and soiling	0.9	
Heliostat availability	0.99	
Image error (slope, single-axis)	1.53	mrad
Reflected image conical error	4.32749	mrad
Number of heliostat facets - X	2	
Number of heliostat facets - Y	8	
Heliostat focusing method	Ideal	

Heliostat Operation

Heliostat stow/deploy angle	8	deg
Wind stow speed	15	m/s
Heliostat startup energy	0.025	kWe-hr
Heliostat tracking power	0.055	kWe
Design-point DNI	950	W/m²

Atmospheric Attenuation

Polynomial coefficient 0	0.006789	
Polynomial coefficient 1	0.1046	1/km
Polynomial coefficient 2	-0.017	1/km²
Polynomial coefficient 3	0.002845	1/km³
Average attenuation loss	3.7	%

A.6 Power Tower and Receiver Parameters

System Design Parameters

Solar multiple	1.40	
Receiver thermal power	42.8	MWt
HTF hot temperature	495.3	°C
HTF cold temperature	290.0	°C

Tower and Receiver Dimensions

Solar field geometry optimization on the Heliostat Field page calculates new values for tower height, receiver height, and receiver diameter.

Tower height	87.8716	m
Receiver height	8.87477	m
Receiver diameter	6.69819	m
Number of panels	20	

Receiver Heat Transfer Properties

Tube outer diameter	40	mm
Tube wall thickness	1.25	mm
Coating emittance	0.88	
Coating absorptance	0.94	
Heat loss factor	1	

Design and Operation

Minimum receiver turndown fraction	0.25	
Maximum receiver operation fraction	1.2	
Receiver startup delay time	0.2	hr
Receiver startup delay energy fraction	0.25	
Receiver HTF pump efficiency	0.850	
Maximum flow rate to receiver	166.479	kg/s

Materials and Flow

HTF type	Salt (60% NaNO3 40% KNO3)
Property table for user-defined HTF	Edit...
Material type	Stainless AISI316
Flow pattern	1

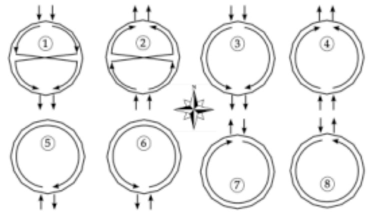

Receiver Flux Modeling Parameters

Maximum receiver flux	1000	kWt/m²
Estimated receiver heat loss	30.0	kWt/m²
Receiver flux map resolution	20	
Number of days in flux map lookup	8	
Hourly frequency in flux map lookup	2	hours

Piping Losses

Piping heat loss coefficient	10200	Wt/m
Piping length constant	0	m
Piping length multiplier	2.6	
Piping length	228.466	m
Total piping loss	2330.35	kWt

A.7 Power Tower System Cost Parameters

Direct Capital Costs

Heliostat Field

Reflective area	129,793 m²	Site improvement cost	16.00	$/m²	$ 2,076,687.12
		Heliostat field cost	170.00	$/m²	
		Heliostat field cost fixed	0.00	$	$ 22,064,800.00

Tower

Tower height	87.8716 m				
Receiver height	8.87477 m	Tower cost fixed	3,000,000.00	$	
Heliostat height	12.2 m	Tower cost scaling exponent	0.0113		$ 8,251,116.00

Receiver

Receiver area	186.752 m²	Receiver reference cost	110,000,000.00	$	
		Receiver reference area	1571	m²	
		Receiver cost scaling exponent	0.7		$ 24,771,622.00

Thermal Energy Storage

Storage capacity	0 MWht	Thermal energy storage cost	26.00	$/kWht	$ 0.00

Power Cycle

Cycle gross capacity	15.27 MWe	Fossil backup cost	0.00	$/kWe	$ 0.00
		Balance of plant cost	340.00	$/kWe	$ 5,191,800.00
		Power cycle cost	1,190.00	$/kWe	$ 18,171,300.00
				Subtotal	$ 80,527,328.00

Contingency

Contingency cost	7	% of subtotal	$ 5,636,913.00
		Total direct cost	$ 86,164,240.00

Indirect Capital Costs

Total land area 199 acres Cycle net (nameplate) capacity 15 MWe

	$/acre	% of direct cost	$/We	$	
EPC and owner cost	0.00	11	0.00	0.00	$ 9,478,066.00
Total land cost	10,000.00	0	0.00	0.00	$ 1,988,692.12

Sales Tax

Sales tax basis	80 % of direct cost	Sales tax rate	0 %	$ 0.00
			Total indirect cost	$ 11,466,758.00

A.8 Financial Input Parameters

Solution Mode

- (●) Specify IRR target
- ( ) Specify PPA price

IRR target	10.29 %	IRR target year	20
PPA price	0.13 $/kWh		

Escalation Rate

PPA price escalation 1 %/year

Inflation does not apply to the PPA price.

Analysis Parameters

Analysis period	25 years	Inflation rate	2.5 %/year
		Real discount rate	7.6 %/year
		Nominal discount rate	10.29 %/year

Tax and Insurance Rates

Federal income tax rate	30 %/year
State income tax rate	0 %/year
Sales tax	0 % of total direct cost
Insurance rate (annual)	0 % of installed cost

Property Tax

Assessed percentage	0 % of installed cost
Assessed value	$ 0.00
Annual decline	0 %/year
Property tax rate	0 %/year

Salvage Value

Net salvage value	5 % of installed cost	End of analysis period value	$ 5,088,953

Project Term Debt

Project Term Debt

- (●) Debt percent 60 % of total cap. cost
- ( ) DSCR 1.3

Choose "Debt percent" to size the debt manually as a percentage of total installed cost. Choose "DSCR" to size the debt based on cash available for debt service. See Help for details.

For a project with no debt, set the either the debt percent or the DSCR to zero.

Tenor	15 years
Annual interest rate	7.78 %
Debt closing costs	450,000.00 $
Up-front fee	2.75 % of total debt
WACC	7.38 %

Be sure to verify that all debt-related costs are appropriate for your analysis: Debt closing costs, up-front fee, and debt service reserve account. Note that debt interest payments are tax deductible, so a project with more debt may have higher net after-tax annual cash flows than a project with less debt.

The weighted average cost of capital (WACC) is displayed for reference. SAM does not use the value for calculations.

Appendix B – Journal Report

Assessing the Potential for CSP Integration with Australia's Coal Fired Power Plants

Joseph O. Somers, 2016
Journal of Renewable and Sustainable Energy

As a result of the high emission intensity and limited supply of fossil fuels, there is a need for Australia to change its focus to renewable energy solutions that have both abundant free energy sources and produce significantly less greenhouse gas emissions. An article released by Dalvi through publication 'Nature Climate Change' [1], titled 'Thermal Technologies as a Bridge from Fossil Fuels to Renewables', details the potential of integrating solar thermal systems to existing Rankine-cycle power plants with minimal modifications to the existing infrastructure. This article will determine the potential of integrating CSP technology with Australia's coal fired power plants. An analysis is performed on the most appropriate solar to coal integration points, the most useful solar collector type for this application, and the resulting PPA price of solar energy produced from an integrated system. It was determined that electricity produced by solar integration is currently more expensive than electricity produced by coal alone, however, it is far more competitive than stand-alone CSP plants. Furthermore, solar-coal integration was found to significantly reduce the CO_2 emissions of a coal-fired power plant.

i. Introduction

Large-scale Concentrating Solar Thermal (CST) systems would be required to add significant energy production to current coal fired plants in Australia. One such system is the power tower model, where thousands of heliostats (large mirrors that track the sun) focus the sun's thermal energy onto a central receiver that in turn heats molten salt to high temperatures. The heated salt is then moved to a thermal storage tank and is eventually pumped into a steam engine, which drives a standard turbine to produce electricity. Similarly, a typical coal-fired power station generates electricity by burning coal in a boiler that heats up water, which is converted into superheated steam. This steam drives a steam turbine that in turn drives a generator that produces electricity. Essentially, the CST plants can be integrated into the current power stations throughout the nation to aid in the reduction of burning of fossil fuels. Integration can either be made into feedwater heating or through supercritical steam in the power cycle [1].

All CSP collectors were analysed and the most viable options for integration to Australia's coal-fired power plants are the power tower and parabolic trough collector systems. Both technologies have high solar concentration and operating temperatures in conjunction with relatively low capital costs. The power tower system has operating temperatures that would be useful for both feedwater heating and direct steam integration to Australia's coal-fired power plants. In comparison, the PTC systems will only be useful for feedwater heating. The Linear Fresnel Reflector system attains reasonably low operating temperatures with its upper temperature limit falling short of the upper bound on feedwater heating. In contrast, parabolic dish collectors have very high operating temperatures, however, this temperature is used directly into a Stirling/Brayton engine. Large heat losses would result if the HTF from the PDC receiver was transported to a heat exchanger to produce steam for integration with coal-fired plants, especially in a utility-scale plant. Furthermore, the capital cost of PDCs are considerably higher than other technologies and they have not been commercially demonstrated.

In a standard coal-fired power plant steam is extracted from the turbines to provide feedwater heating for the boiler. In the proposed integrated system, molten salt carrying solar energy, which is produced in the CSP plant, replaces the extraction steam to heat the feedwater and the steam thus saved can continue to do work (as detailed in figure 1). As the solar heat does not enter the turbine, the efficiency of solar to power is not limited by the temperature of the solar heat [13].

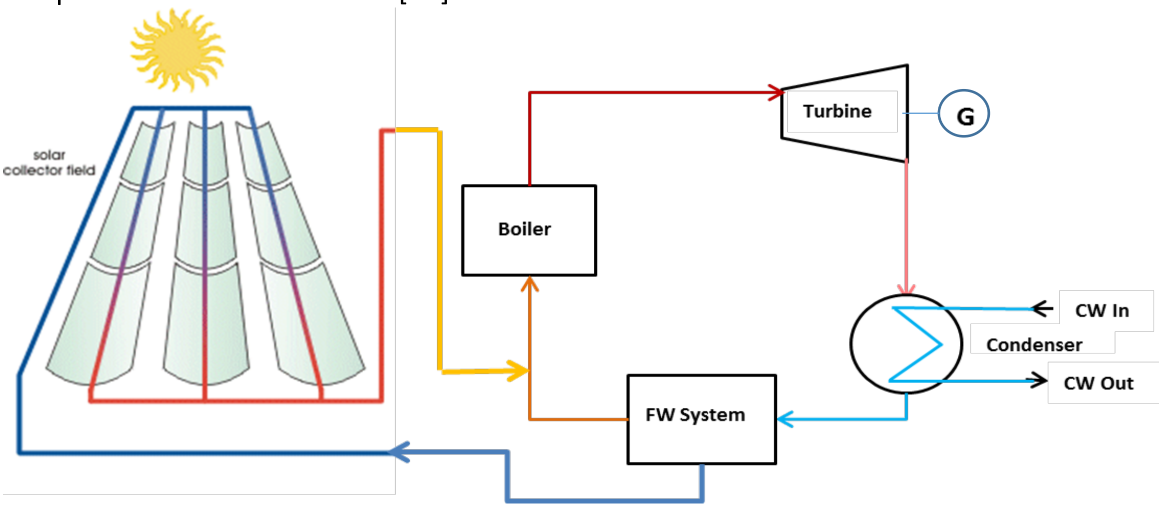

Figure 1. Feedwater Integration

Figure 2 below details a simplified version of the feedwater heating section in a conventional coal-fired power plant. A report by Hongjuan [13] in 2012 titled 'Solar-Coal Hybrid Thermal Power Generation', explains that as a result of thermodynamic factors, only feedwater inputs 1 and 2 are economically feasible to use solar fields for their heating. The report goes on to explain that each feedwater input requires its own solar field to be optimised and have the output fluid temperature of the field be equal to the extraction steam temperature that would otherwise be utilised [13]. As a result of this, the remainder of this report will focus on analysis of solar fields for both 'feedwater input 1' and 'feedwater input 2'.

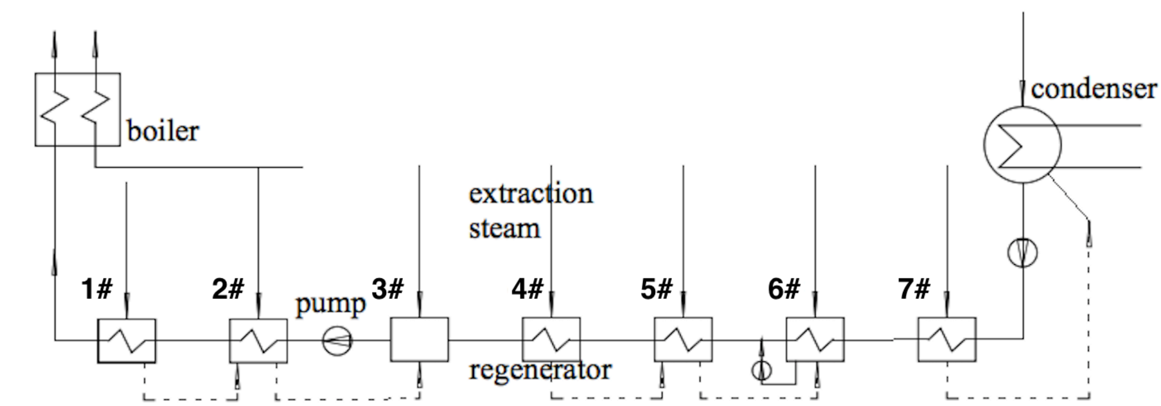

Figure 2. Feedwater Component of a Coal-Fired Power Plant

Table 1 details the coal-fired power plants that were used for analysis and the mean DNI at the closest available solar resource.

Table 1. Coal-Fired Power Plants for Analysis

Power Station	**Location**	**Capacity (MW)**	**Type of Coal Used**	**Closest Solar Resource**	**Mean DNI at resource $\left(W/_{m^2}\right)$**
Stanwell	QLD	1445	Black	Chinchilla, QLD	268
Vales Point	NSW	1320	Black	Sydney, NSW	166
Yallourn	VIC	1480	Brown	Melbourne, VIC	134

ii. Model

The performance of the integrated system was analysed using the System Advisory Model (SAM), a CSP analysis tool produced by the National Renewable Energy Laboratory (NREL). SAM makes 'performance predictions and cost of energy estimates for grid-connected power projects based on installation and operating costs and system design parameters that you specify as inputs to the model' [21]. SAM utlisies the annual DNI data for a given location to both size and provide annual cost and capacity data for a solar power plant. Once a model is produced, SAM allows for parametric analysis of every variable that has been entered, allowing for efficient optimization of the system.

One of the most important input metrics to SAM is the gross power output of the desired solar power plant. In this model, the solar field is required to produce enough steam to replace the amount turbine extracted steam at each feedwater input. Therefore, the amount of heat the solar plant needs to produce is equal to the amount of heat provided from the extraction steam. The amount of heat provided by the extraction steam can be calculated from thermodynamic principles.

$$m_s = \frac{q}{h_e} \qquad (1)$$

Where; m_s(kg/s) is the mass flow rate of the steam, q (kJ/s) is the mean heat transfer rate, and h_e (kJ/kg) is the evaporation heat of steam at a given pressure. An arbitrary cycle conversion efficiency value 0.5 is inputted to the model. This tricks SAM into thinking the solar field is connected to a turbine that is 50% efficient, which despite being higher than standard turbines, it still allows the simulations to run without error.

Table 2 below details the 'gross power output' required from each feedwater heating point from each coal-fired power station being used for analysis. The 'gross power outputs' listed in the final column of table 5.1, were then used as inputs to SAM to size each solar field.

Table 2. Gross Power Output Calculations for SAM

Power Station	Feedwater Input	Mass Flow Rate of Steam (m_s − kg/s)	Pressure of Steam (kPa)	Evaporation Heat of Steam (h_e − kJ/kg)	Heat Provided by Steam (q − MW)	Gross Power Output for SAM (MW)
Stanwell	1	23.235	4165	1704	39.6	**19.8**
	2	16.254	2109	1878	30.5	**15.3**
Vales Point	1	45.39	4196	1700	77.2	**38.6**
	2	29.21	2098	1878	54.8	**27.4**
Yallourn	1	21.951	4101	1708	37.5	**18.8**
	2	14.595	1955	1896	27.7	**13.8**

An optimal parabolic trough and power tower field was then inputted to SAM separately and analysed. The financial parameters in this analysis were used to emulate the Australian tax system, and were suggested by the Australian Solar Thermal Energy Association [22]. The financial parameters used in both the parabolic trough and power tower modelling are detailed in table 3 below. No governments incentives were included in the modelling.

Table 3. Financial Input Parameters for SAM

Financial Parameter	Input to SAM
IRR Target	10.29%
IRR Target Year	20 years
PPA Price Escalation Rate	1 %/year
Analysis Period	25 years
Inflation Rate	2.5%
Real Discount Rate	7.6%
Nominal Discount Rate	10.29%
Federal Income Tax Rate	30%
State Income Tax Rate	0%
Net Salvage Value	5% of installed cost
Property Tax	0% of installed cost
Loan: Debt Percent	60% of total capital cost
Loan: Tenor	15 years
Loan: Annual Interest Rate	12%

iii. Results

Beyond parameters that cannot be changed such as the location and DNI resource, the most vital parameter in sizing a solar field is the solar multiple. 'The solar multiple is a measure of the solar field aperture area as a function of the power block's nameplate capacity' [23]. Increasing the solar multiple of a solar farm increases its capacity factor allowing it to operate at capacity for longer, however, it also increases the amount of heat energy dumped during high irradiation periods [23]. As such an optimal level must be found which minimises the cost of heating in cents/kWh. A parametric analysis on solar multiple was performed, and the optimal level and resulting PPA price of heating is detailed in table 4.

Table 4. Final SAM Outputs

Power Plant	Feedwater Input	Collector Type	Solar Multiple	Annual Heating Output (GWh)	Capacity Factor (%)	PPA Price of Heating (cents/kWh)
Stanwell Mean DNI = 268.2 (W/m^2)	Feedwater 1	Parabolic Trough	2.6	104.6	30.2	**6.21**
		Power Tower	1.4	81.7	23.6	**12.96**
		Difference (Trough-Tower)	-	22.9	6.6	**-6.75**
	Feedwater 2	Parabolic Trough	1.4	59.5	22.3	**5.56**
		Power Tower	1.4	63	23.5	**14.15**
		Difference (Trough-Tower)	-	-3.5	-1.2	**-8.59**
Vales Point Mean DNI = 165.8 (W/m^2)	Feedwater 1	Parabolic Trough	2.6	129.5	19.2	**9.69**
		Power Tower	1.4	105.2	15.6	**17.80**
		Difference (Trough-Tower)	-	24.3	3.6	**-8.11**
	Feedwater 2	Parabolic Trough	1.4	59.3	12.3	**9.72**
		Power Tower	1.4	74.9	15.6	**18.68**
		Difference (Trough-Tower)	-	-15.6	-3.3	**-8.96**
Yallourn Mean DNI = 134 (W/m^2)	Feedwater 1	Parabolic Trough	2.6	50.5	15.4	**12.18**
		Power Tower	2.2	43.8	13.3	**28.53**
		Difference (Trough-Tower)	-	6.7	2.1	**-16.35**
	Feedwater 2	Parabolic Trough	1.8	25.7	10.6	**13.55**
		Power Tower	2.2	30.7	12.7	**32.00**
		Difference (Trough-Tower)	-	-5	-2.1	**-18.45**

It is clear from table 4 that in every simulation the PTC system is a more economically competitive solution when compared to the power tower model. This is largely due to the fact that the capital cost of power tower systems is substantially higher when compared to PTCs, however, this increase in cost results in little, if any, gains on heat energy produced and capacity factor (see section 6.3).

Next the cost of electricity that the steam left un-extracted would produce when the solar farm is providing the heating for the feedwater was calculated. The annual electricity produced from the un-extracted steam can be calculated using the following equation:

$$Electricity\ from\ steam_{annual} = \dot{m}\times(h_i - h_o)\times365days\times24hours\times Gen_{eff}\times CAPF \quad (2)$$

Where;
$\dot{m}$ = mass flow rate of steam $\left(kg/_{s}\right)$,
h_i = Input enthalpy of the steam $\left(kJ/_{kg}\right)$,
h_o = Output enthalpy of the steam after passing through the turbine $\left(kJ/_{kg}\right)$,
Gen_{eff} = Generator efficiency of the coal-fired power plant,
$CAPF$ = Capacity factor of the PTC plant,
$Electricity\ from\ steam_{annual}$ = Electricity produced by un-extracted steam (kWh).

Now, to determine the cost of electricity (in cents/kWh) produced from the solar farm, the following equation can be used:

$$Solar_{cost} = \frac{Annual\ levelised\ heating\ cost\ from\ solar}{Electricity\ from\ steam_{\ annual}} \quad (3)$$

Table 5 details all parameters of the last two equations which are used to calculated the cost of energy produced by the solar field.

Table 5. Solar Electricity Cost

Power Plant	**Stanwell**		**Vales Point**		**Yallourn**	
Feedwater Input	1	2	1	2	1	2
Extraction Steam Mass Flow Rate (kg/s)	23.235	16.254	45.39	29.21	21.951	14.595
Steam Enthalpy Input (kJ/kg)	3532.5	3368.1	3532	3375	3533	3350
Steam Enthalpy Output (kJ/kg)	2372.3		2384		2398	
Generator Efficiency (%)	98.8		99		98.8	
Solar Plant Capacity Factor (%)	30.2	22.3	19.2	12.3	15.4	10.6
Annual Electricity from Steam (GWh)	52.30	31.24	86.59	30.82	33.21	12.75
Annual Levelised Cost of Solar Heating ($ million)	6.5	3.311	12.56	5.763	6.148	3.476
Solar Electricity Cost (cents /kWh)	**9.22**	**10.6**	**14.5**	**18.7**	**18.5**	**27.3**

The cost of producing electricity from coal varies depending on the fluctuating price of coal, however, an average value of $4\ \frac{cents}{kWh}$ is attained from the Australian Bureau of Resources and Energy Economic (BREE) [25]. Clearly, none of the integrated solar power plants attains this value, with the closest integrated plant 'feedwater 1 integration in Stanwell' attaining a price that is just over twice as expensive. This makes the solar integration system economically less appealing when compared to leaving the coal plant to operate as normal. It is important to note that if the Australia government were to introduce a carbon tax or emissions trading scheme, then the price of electricity production from coal would inevitably increase. In this case, this solar integration cost would become more competitive as a result of its low emissions.

Finally, an environmental analysis was performed. An annual report by the 'National Greenhouse and Energy Reporting' (NGER) government clean energy regulator details figures on the amount of CO_2 emissions each coal-fired power station in Australia produced in 2014 [28]. The total amount of avoided CO_2 emissions from the proposed integrated plant can be calculated by multiplying this intensity factor by the amount of annual electricity saved because of the heating provided by each PTC field. The results are displayed below in table 6.

Table 6. Environmental Analysis

Power Station	Feedwater Input	Annual Solar Electricity Produced (MWh)	Power Station Coal Type	Power Station Emission Intensity $(tonnesCO_2/MWh)$	CO_2 avoided (tonnes)	Percent of total Annual Power Plant Emissions (%)
Stanwell	1	52,300	Black Coal	0.86	44,978	0.87
	2	31,240			26,866	0.52
	Total	83,540			71,844	1.39
Vales Point	1	86,590	Black Coal	0.87	75,333	1.44
	2	30,820			26,814	0.51
	Total	117,410			102,147	1.95
Yallourn	1	33,120	Brown Coal	1.27	42,062	0.55
	2	12,750			16,193	0.21
	Total	45,870			58,255	0.76

iv. Conclusion

The following conclusions were reached from this investigation:

- Parabolic trough collector systems are the most useful and cost effective solar collector type for this application.
- Feedwater heating integration is the most cost effective solar input into Australia's coal fired power plants.
- Each power plant's DNI resource is the most crucial factor in determining the feasibility a proposed solar integration project.
- Electricity produced by solar integration is currently more expensive than electricity produced by coal alone, however, it is far more competitive than stand-alone CSP plants.
- Solar-coal integration plants could be used as an effective means of emissions reduction.

Figure 3 details the relationship between the mean DNI at each analysed coal-fired power station and the resulting solar electricity PPA price. A negative-power trend line has been fitted to the data. This relationship will be used to extend this investigation to Australia's coal-fired power plants that were not analysed.

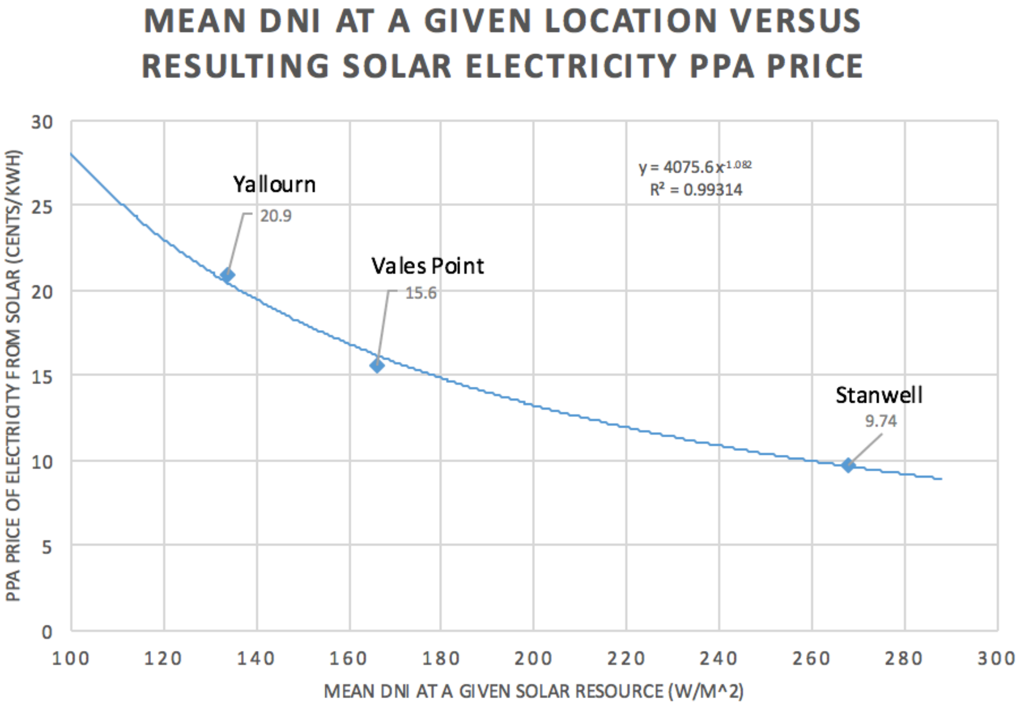

Figure 3: Mean DNI at a Given Solar Location Versus Resulting Solar Electricity PPA Price

The trend line equation from figure 3 was used to calculate the expected PPA price of solar electricity if integration were to occur at each coal-fired power station in Australia. Each coal-fired power station in Australia has also been given a 'solar integration potential' rating depending on the estimated PPA price of its resulting solar electricity: less than 10cents/kWh = Excellent, between 10 and 15 cents/kWh = good, between 15 and 20 cents/kWh = fair, and over 20 cents/kWh = poor. The results indicated that coal-fired power plants located in Queensland and South Australia attain an 'excellent' score, plants in Western Australia attain a 'good' score, plants in New South Wales attain a 'fair' score, and finally plants in Victoria were considered to have 'poor' solar integration potential.

These estimates are rough, and are based solely on the power plants mean DNI data at the closest location with solar data available. It would be beneficial for this table to be updated with more accurate solar resource data if these become available in the future. Furthermore, as seen in this report, numerous other factors affect the PPA price of electricity modelling such as; plant capacity, power plant configuration and efficiencies, and feedwater extraction steam properties. Therefore, the solar integration potential should only be used as an indication as to whether further, more complete analysis should be performed on each power plant using the methods carried out in this article for Stanwell, Vales Point, and Yallourn power stations.